Measurements of Higgs boson production and decay rates and their interpretation with the ATLAS experiment

Mark Owen
The University of Glasgow
12 January 2023, HEP2023, Valparaiso, Chile

Introduction

- The Higgs boson sits at the heart of the Standard Model.
  - Potentially linked to fundamental unanswered questions & new physics that may provide the answers:

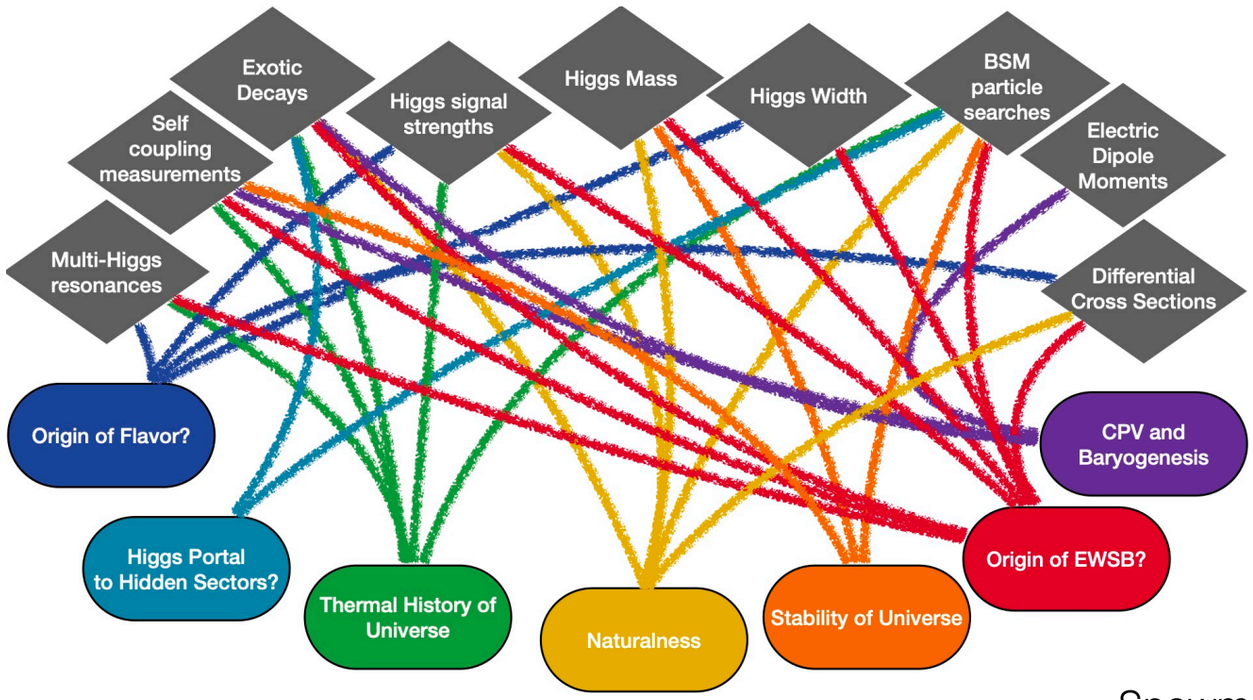

Snowmass: arXiv:2209.07510

- Since discovery in 2012, 100+ ATLAS papers across all decay & production modes.
- Overall goal is precision measurements to search for deviations from SM predictions.
- Discuss today recent highlights of the cross-section & coupling measurements.

Introduction

- The Higgs boson sits at the heart of the Standard Model.
  - Potentially linked to fundamental unanswered questions & new physics that may provide the answers:

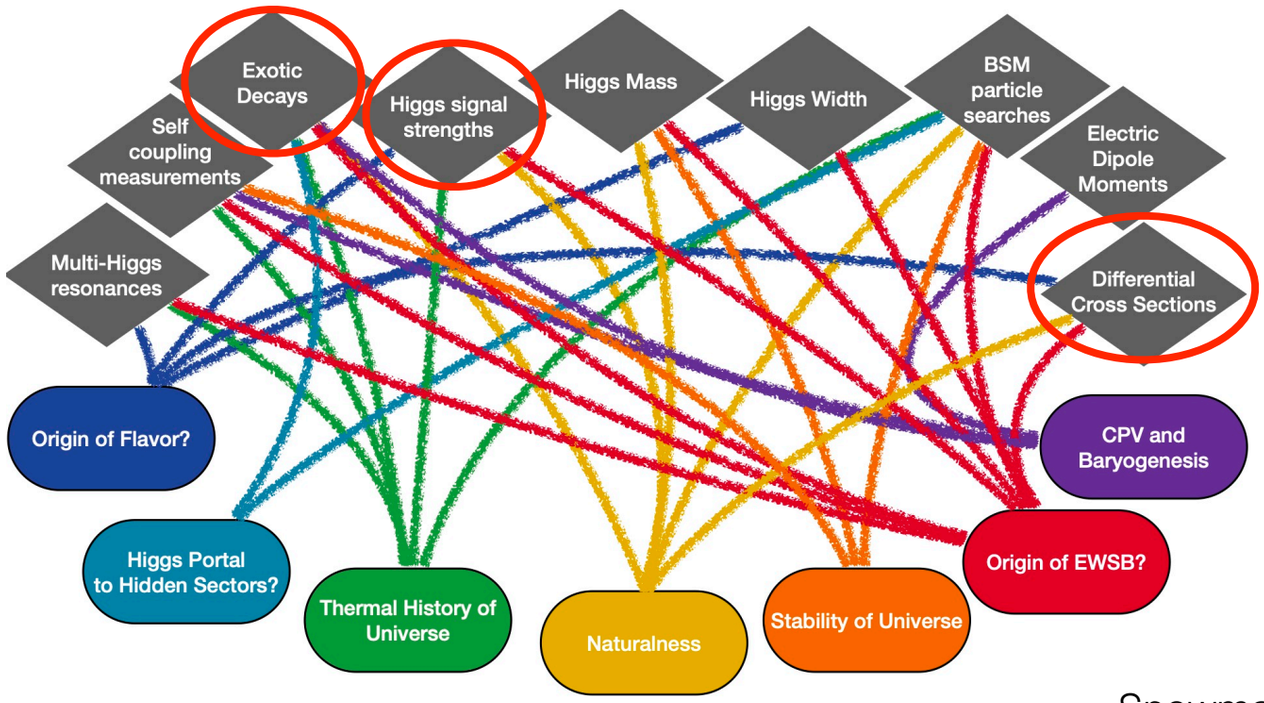

Snowmass: arXiv:2209.07510

- Since discovery in 2012, 100+ ATLAS papers across all decay & production modes.
- Overall goal is precision measurements to search for deviations from SM predictions.
- Discuss today recent highlights of the cross-section & coupling measurements.

Higgs couplings

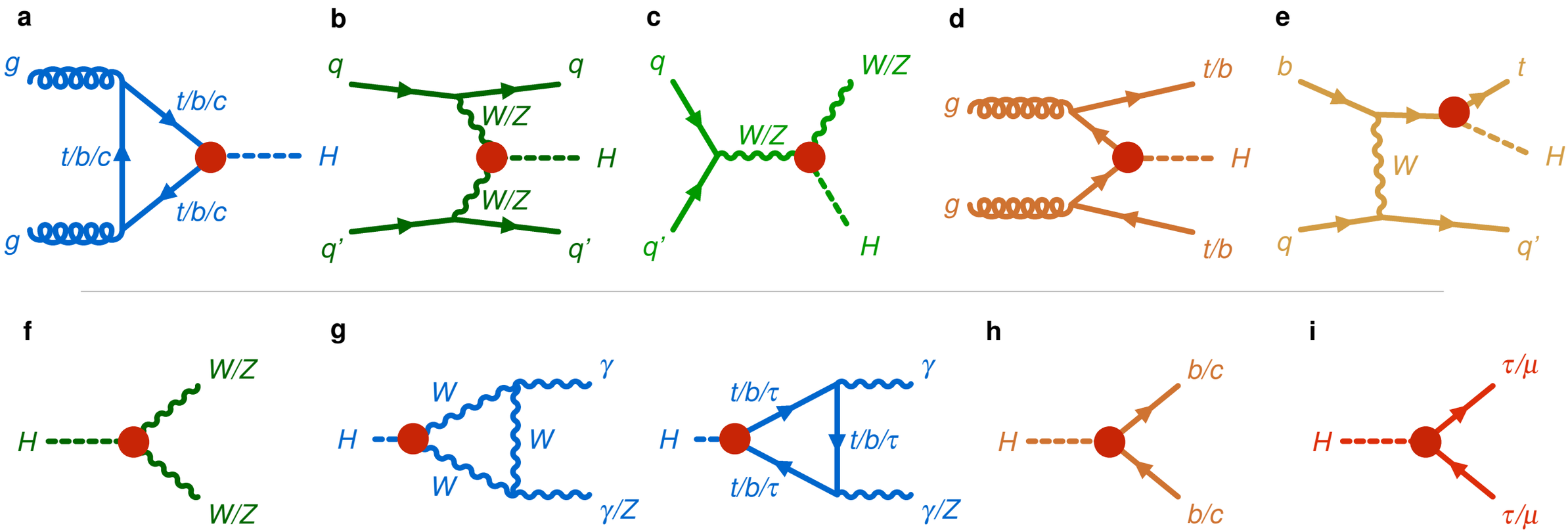

- New physics can appear in any / all of the production / decay modes.
- Need systematic ways to examine deviations from the SM.

Interpreting Higgs data

- Measurements:
  - Inclusive cross-section measurements of particular production & decay mode, e.g. gluon-fusion with $H \to WW$.
  - Simplified template cross-sections (STXS): split data into multiple kinematic regions and measure cross-section in each region. Regions designed to optimise BSM sensitivity.
  - Differential cross-sections: measure fiducial cross-sections differentially to minimise model dependence.
- Interpretations:
  - Signal strengths: measure the rate of each process (production x decay) compared to the SM prediction.
  - Coupling measurements: individual couplings in the SM are assumed to be modified with κ_i factors. SM: $\kappa_i = 1$.
    - As more κ_i are added - less (SM-like) assumptions.
  - Effective field theory: use measured data to constrain any (high energy scale) new physics model.

$$\mathcal{L}_{\text{EFT}} = \mathcal{L}_{\text{SM}} + \sum_{i,D} \frac{C_i^D}{\Lambda^{D-4}} O_i^D,$$

Outline

- Discuss three recent measurements:
  - $H \to \gamma\gamma$
  - $VH(\to WW)$
  - $VH(\to c\bar{c})$
- Then present combined constraints from combination across all channels.

$H \to \gamma\gamma$

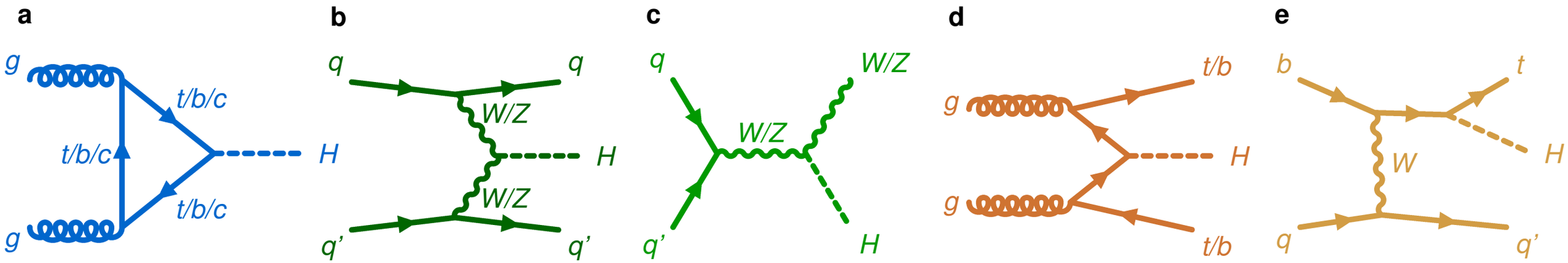

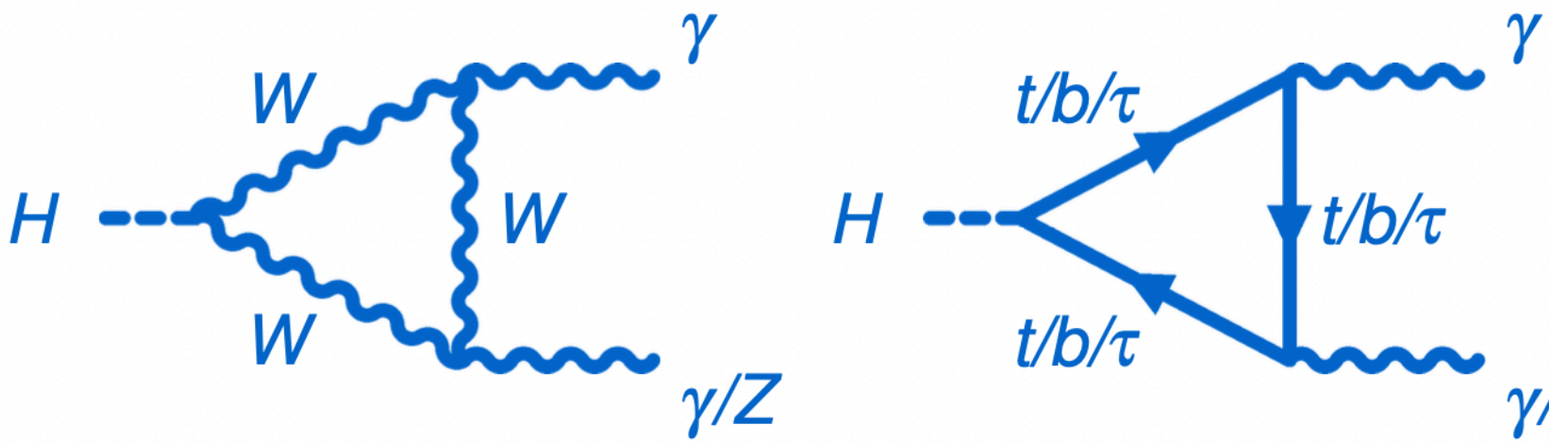

- Events must contain two photons and a multiple BDTs are used to assign events into 101 different analysis categories related to 28 STXS categories.

arXiv:2207.00348

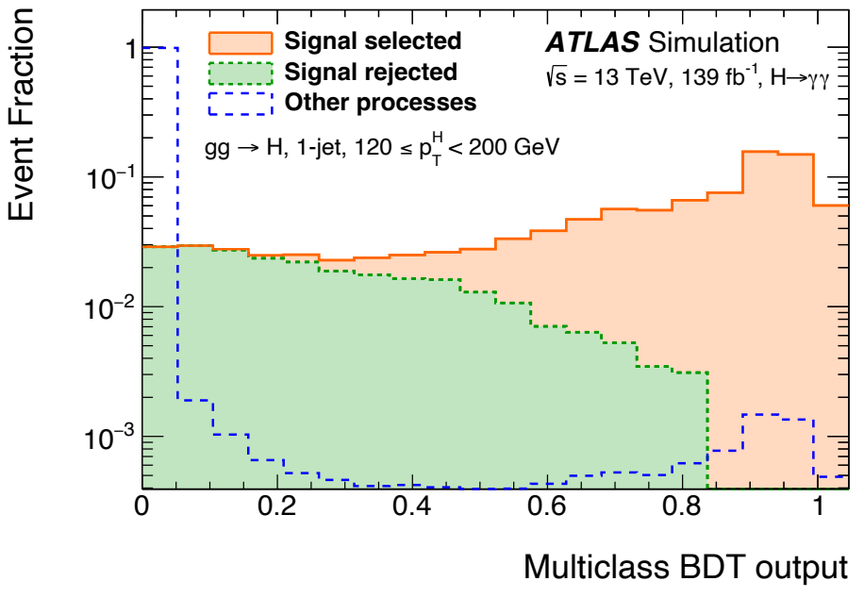

$gg \to H$, 1-jet, $120 \leq p_{\mathrm{T}}^{H} \leq 200\,\mathrm{GeV}$

$H \to \gamma\gamma$

- Fit performed on $m_{\gamma\gamma}$ distribution in each region:

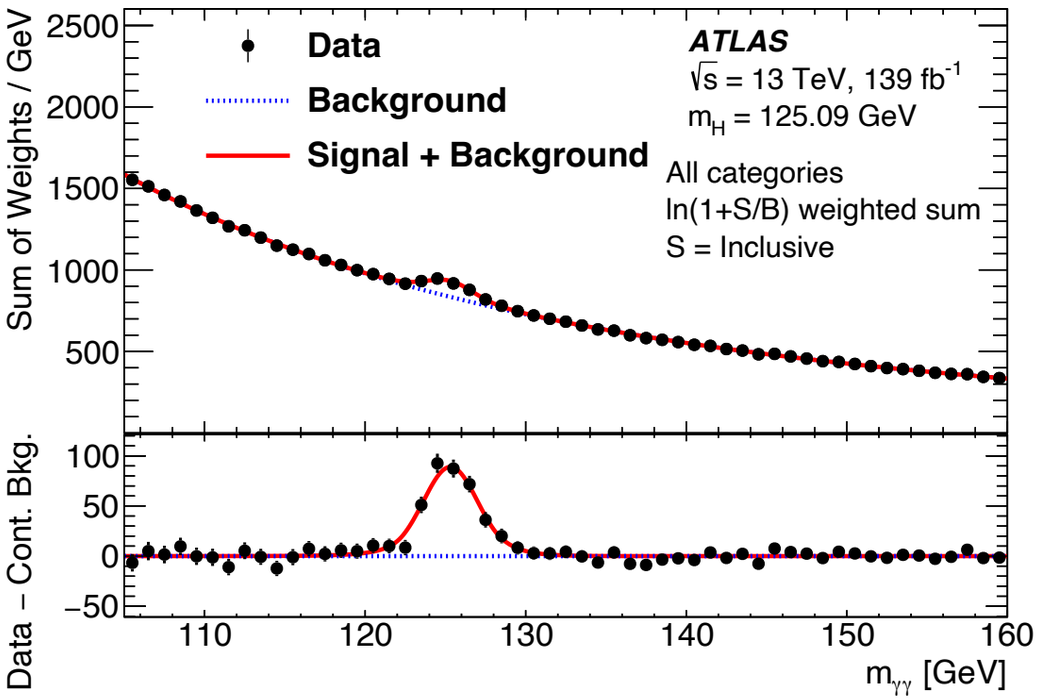

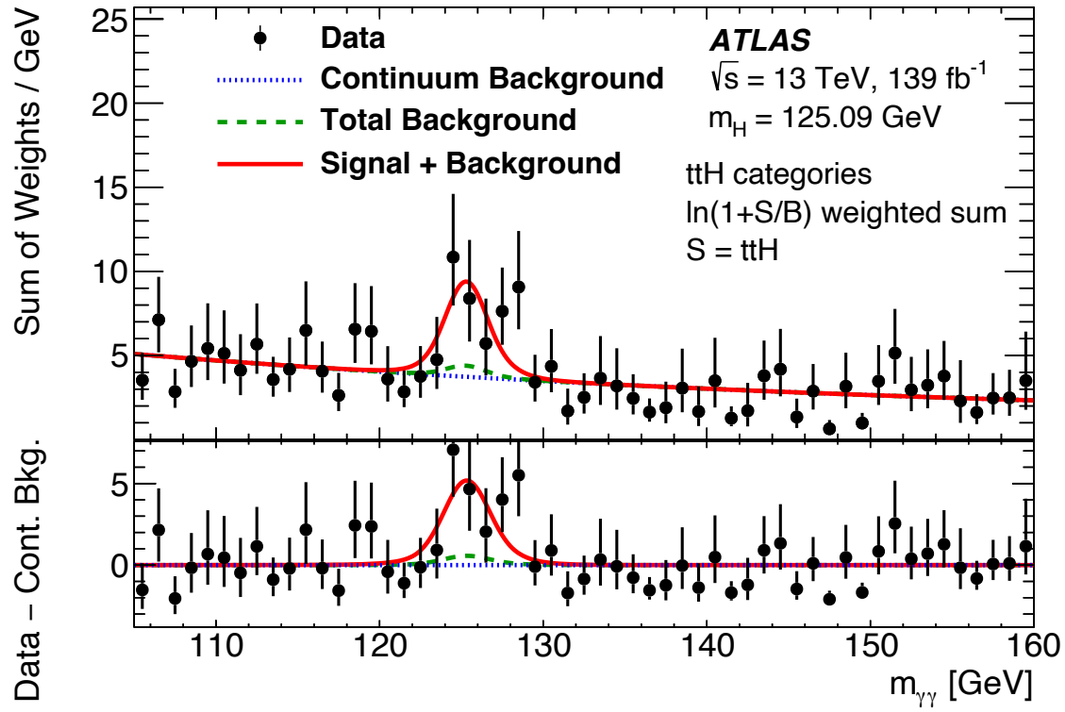

arXiv:2207.00348

$H \to \gamma\gamma$

- Fit performed on $m_{\gamma\gamma}$ distribution in each region:

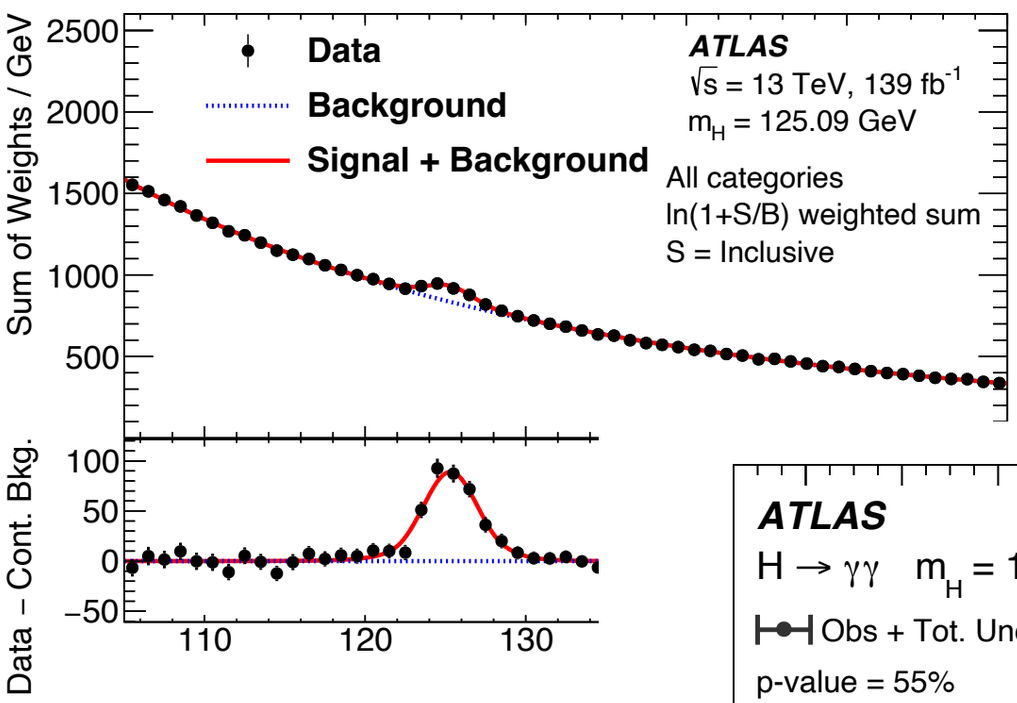

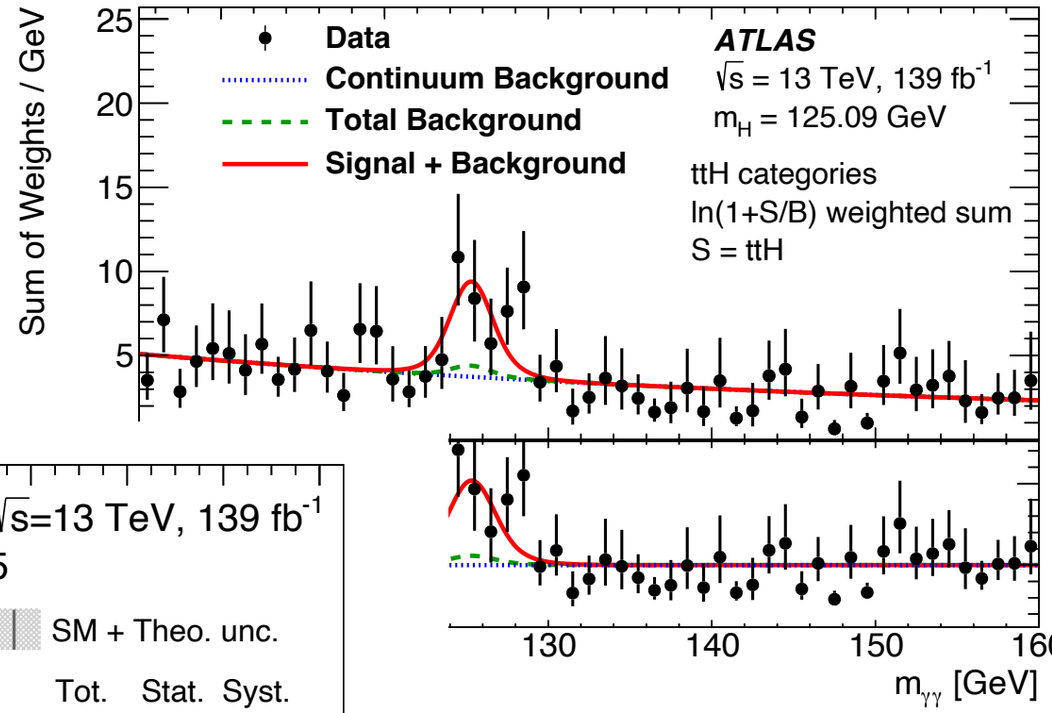

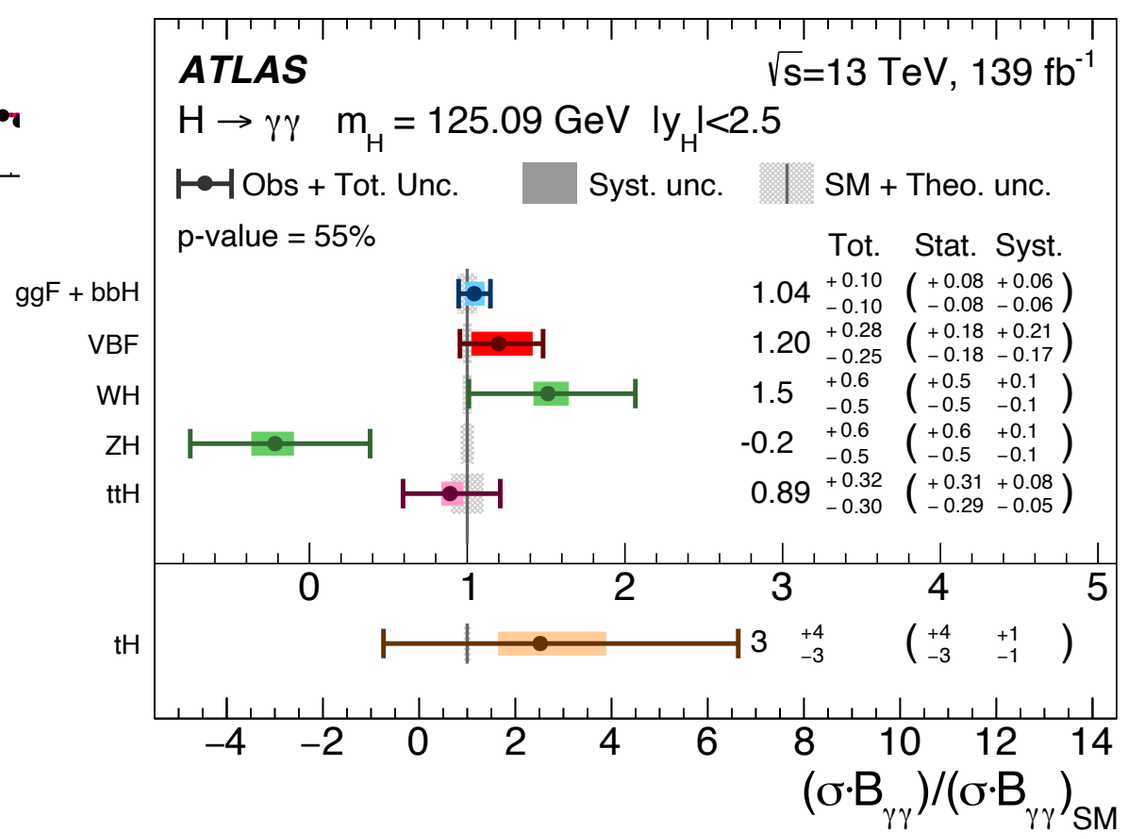

arXiv:2207.00348

$H \to \gamma\gamma$ STXS

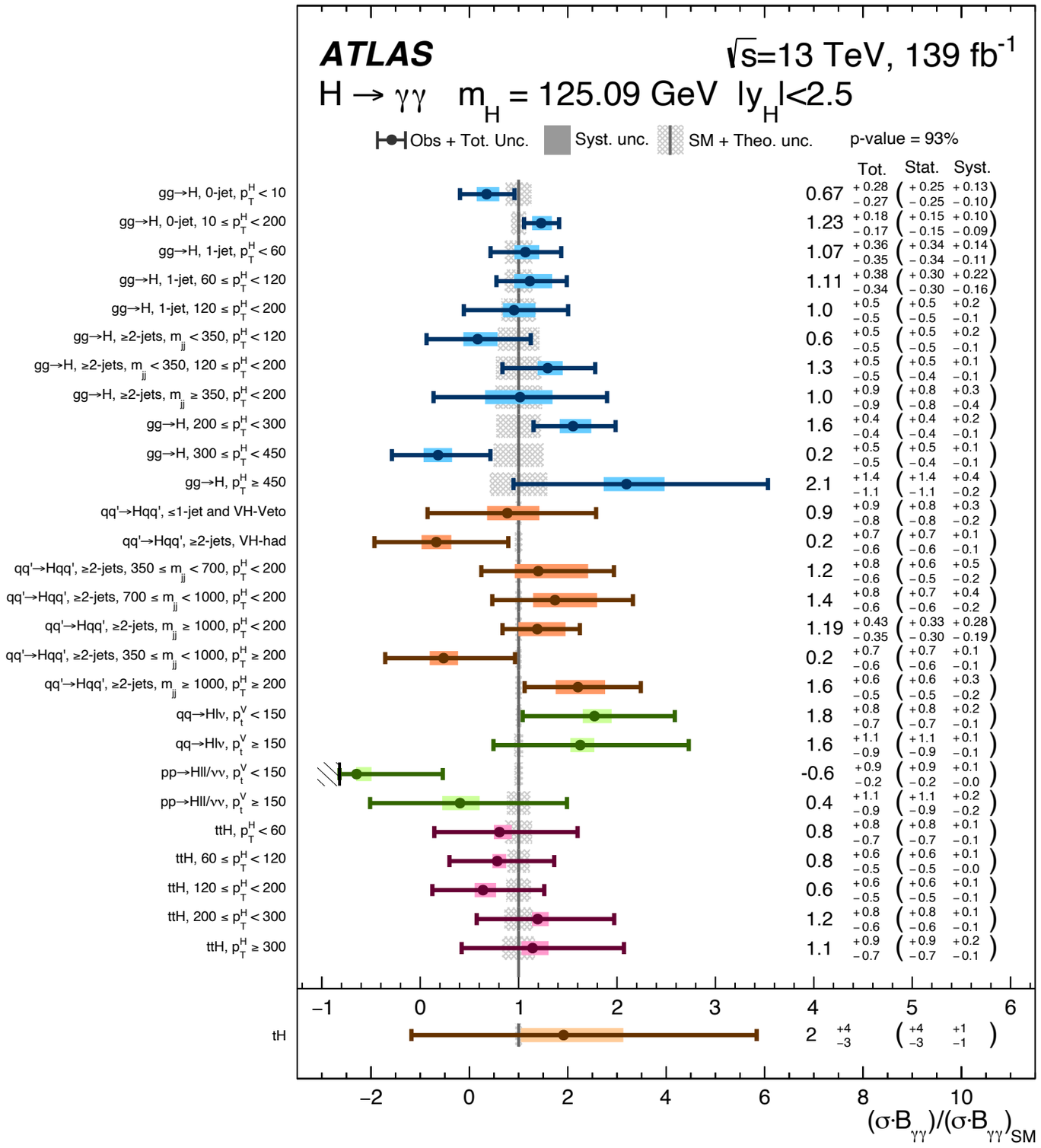

- Statistical uncertainties dominate - looking forward to run-3 data!

arXiv:2207.00348

$H \to \gamma\gamma$ Kappa

- tH region allows to distinguish sign of κ_t:

$$\sigma_i \cdot B_{\gamma\gamma} = \frac{\sigma_i(\kappa) \cdot \Gamma_{\gamma\gamma}(\kappa)}{\Gamma_H(\kappa)}$$

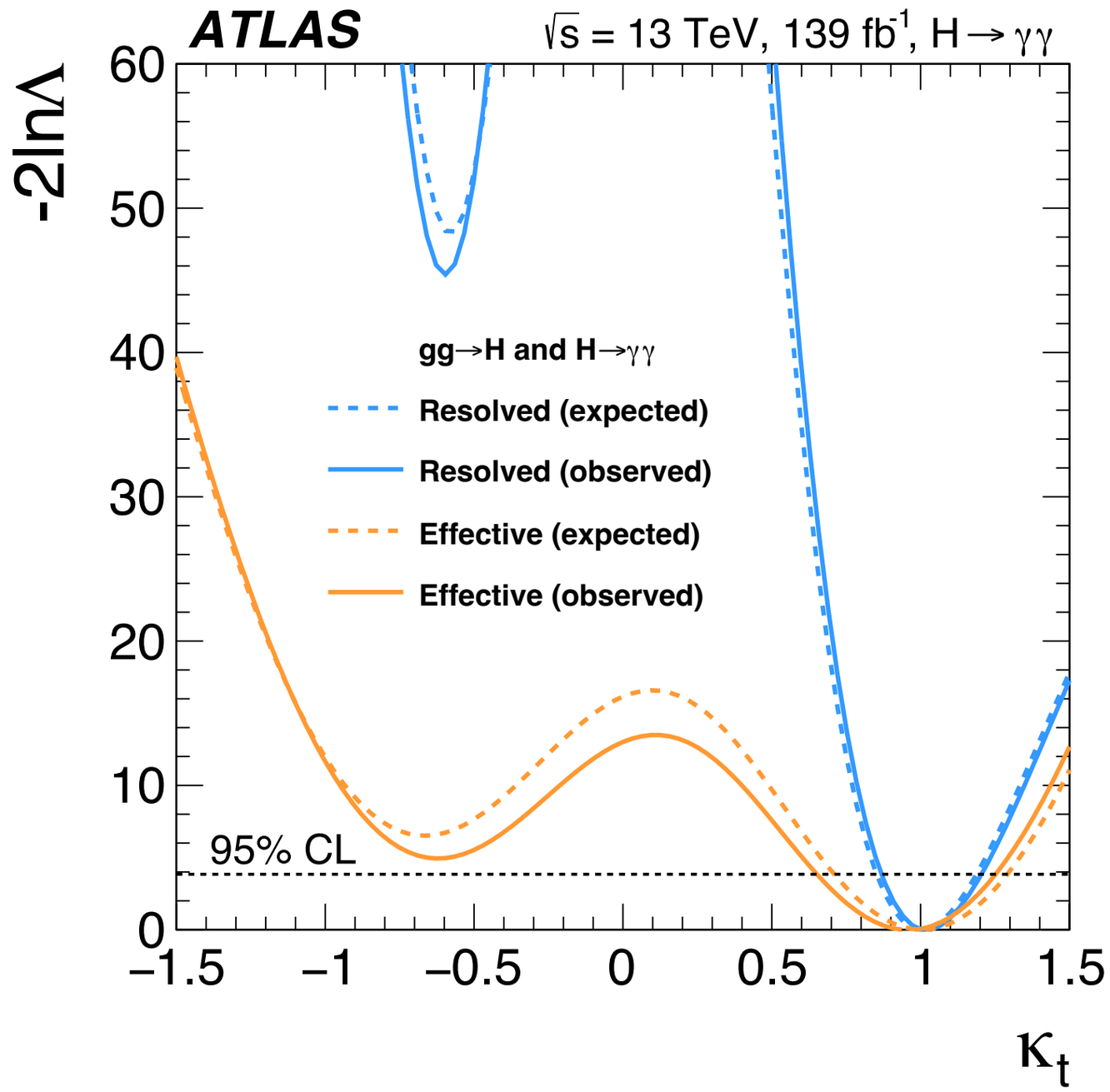

arXiv:2207.00348

$VH; H \rightarrow WW$

- Recent measurement targeting WH and ZH with $H \rightarrow WW$.

- Measurement uses events with 2, 3 or 4 leptons:

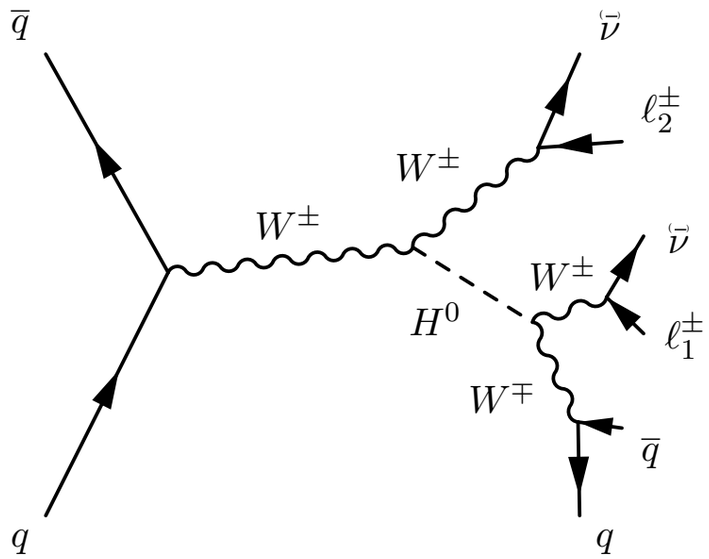

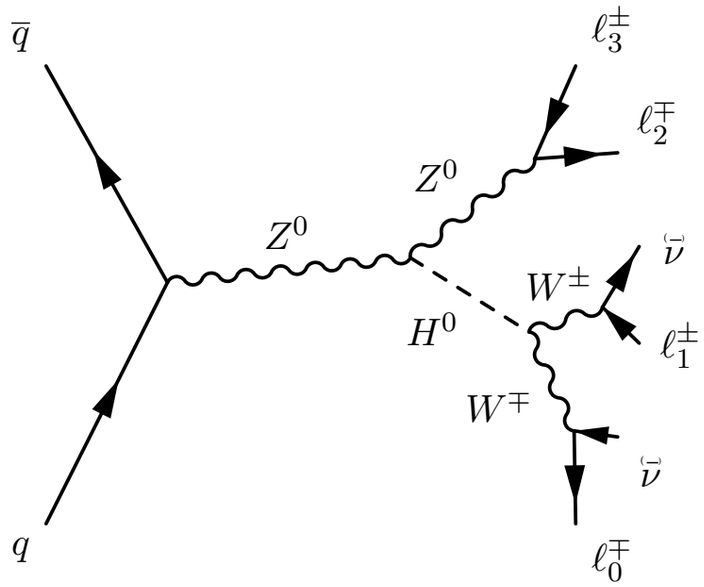

- Signal is differentiated from background with multi-variate techniques (NN or BDT).

- 3l gives best sensitivity to WH and 4l gives best sensitivity to ZH.

- Control regions used to constrain dominant backgrounds.

ATLAS-CONF-2022-067

$VH; H \rightarrow WW$

- 3l & 4l events split according to number of same-flavour opposite-sign-charge lepton pairs:

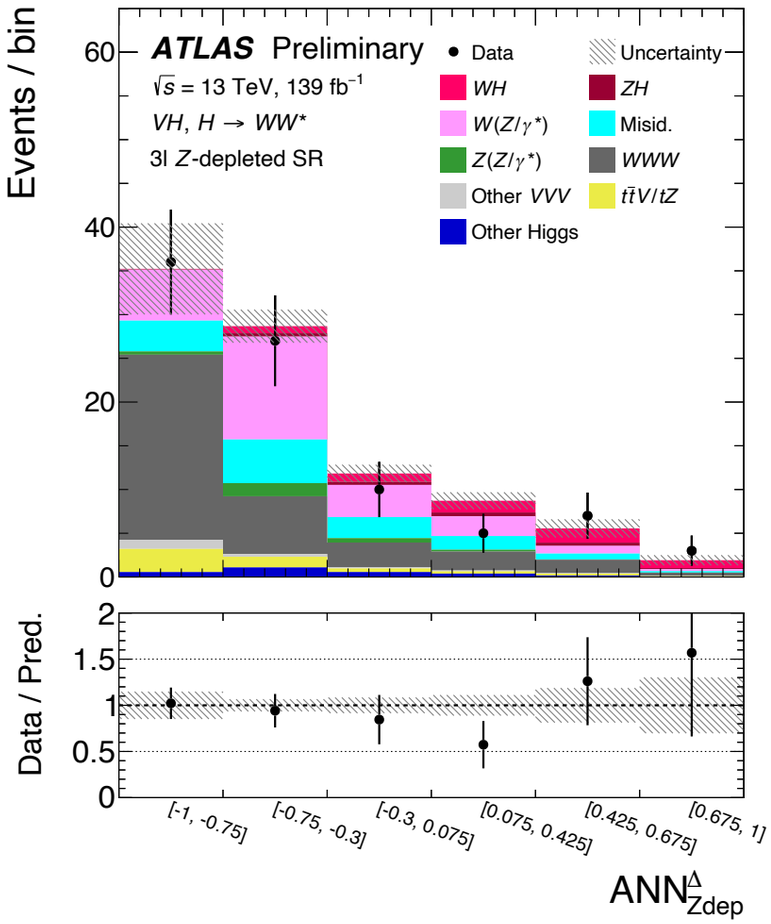

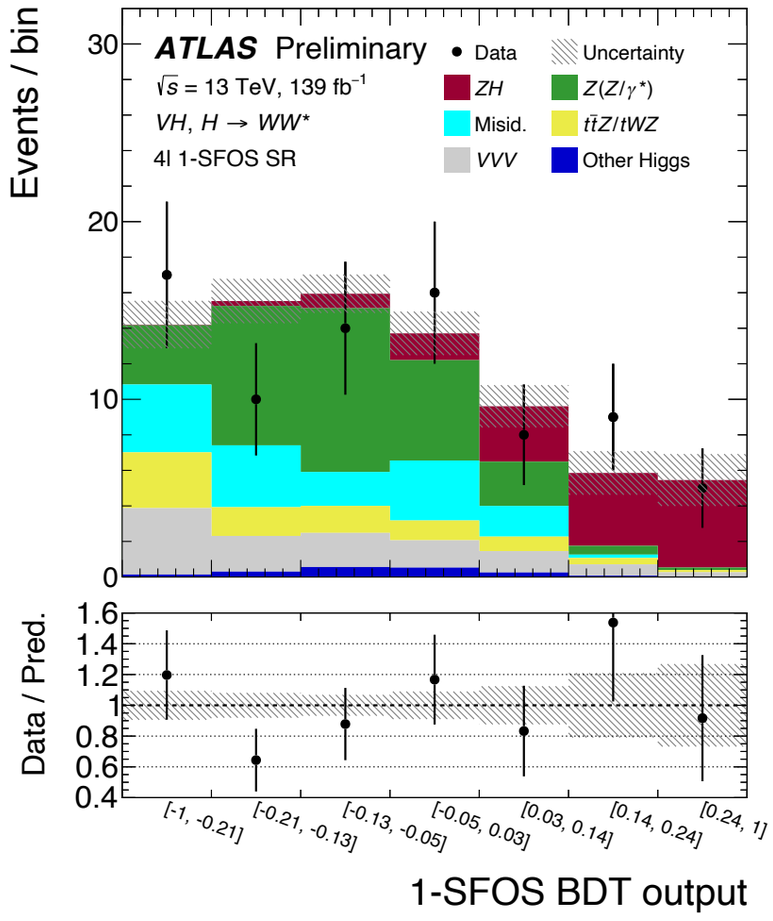

ATLAS-CONF-2022-067

$VH; H \rightarrow WW$

- 3l & 4l events split according to number of same-flavour opposite-sign-charge lepton pairs:

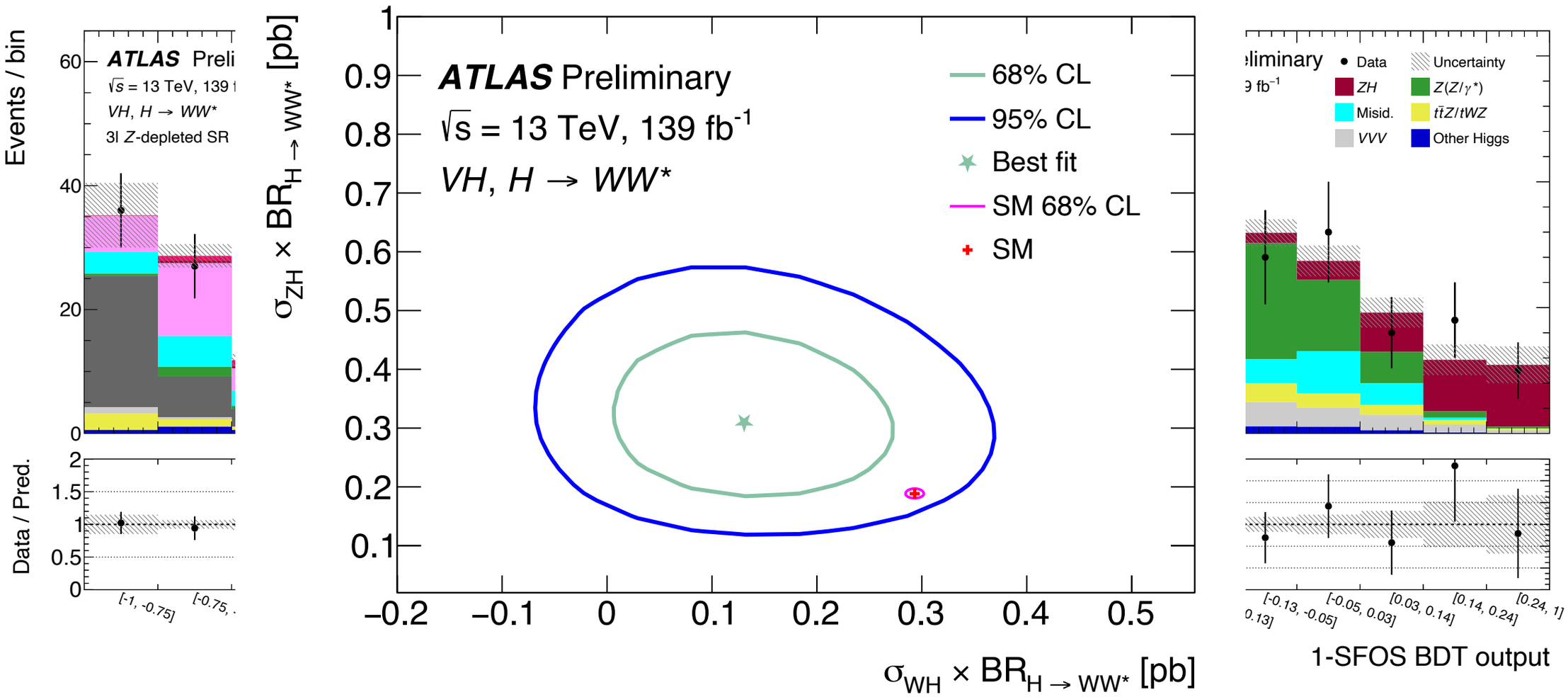

- Analysis shows 4.6σ evidence for VH production and measurements are statistics limited.

ATLAS-CONF-2022-067

$H \to c\bar{c}$

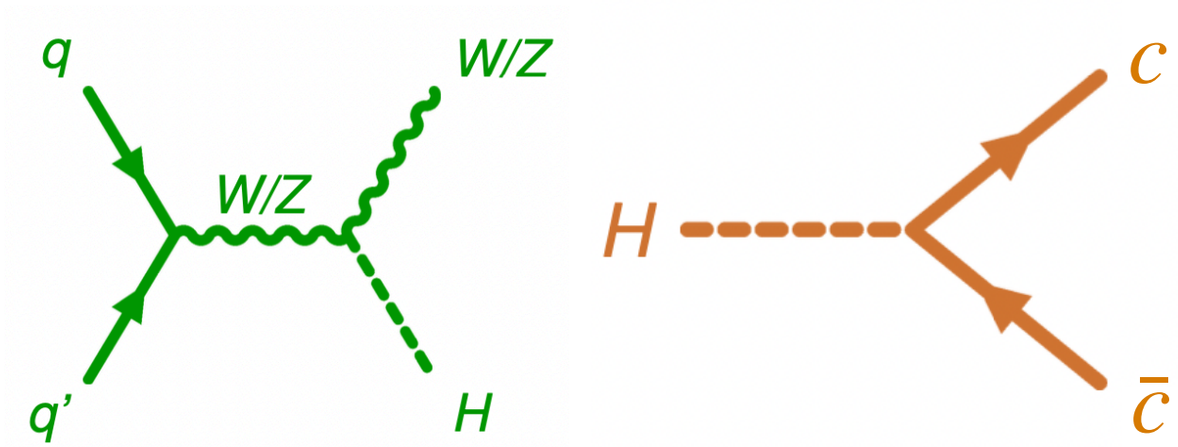

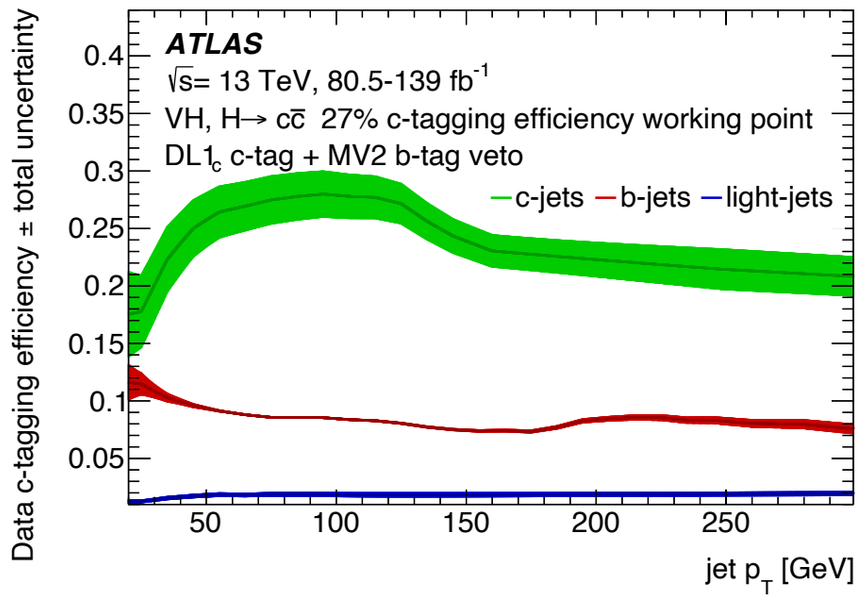

- Low BR (2.9%) and large backgrounds make signal extraction highly challenging.

- VH search is performed simultaneously with measurement of $VW(\to cq)$ and $VZ(\to c\bar{c})$.

- 16 signal regions defined with p_T^V > 150 GeV (75 GeV in 2 lepton) covering events with 0, 1, 2 leptons, jet multiplicity & number of c-tagged jets.

- Control regions are used for V+jets and top-quark backgrounds.

EPJC 82 (2022) 717

$H \to c\bar{c}$

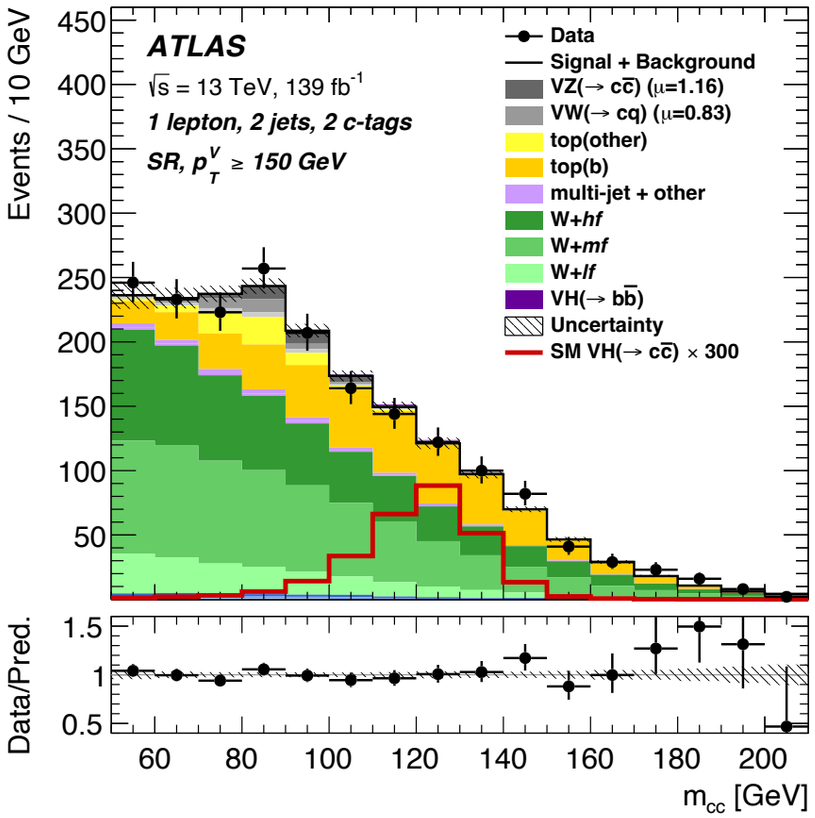

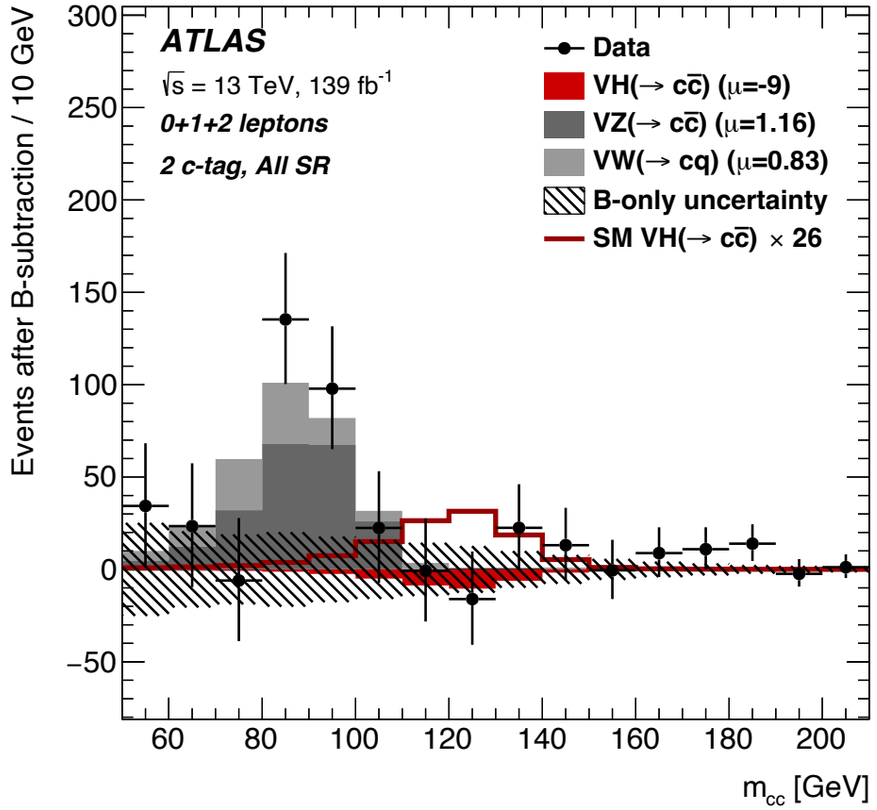

$$\mu_{VW(cq)} = 0.83 \pm 0.11\ (\text{stat.}) \pm 0.21\ (\text{syst.})$$

$$\mu_{VZ(c\bar{c})} = 1.16 \pm 0.32\ (\text{stat.}) \pm 0.36\ (\text{syst.}).$$

$$\mu_{Hc\bar{c}} < 26 \quad \left(31^{+12}_{-8}\right)$$

EPJC 82 (2022) 717

$H \to c\bar{c}$

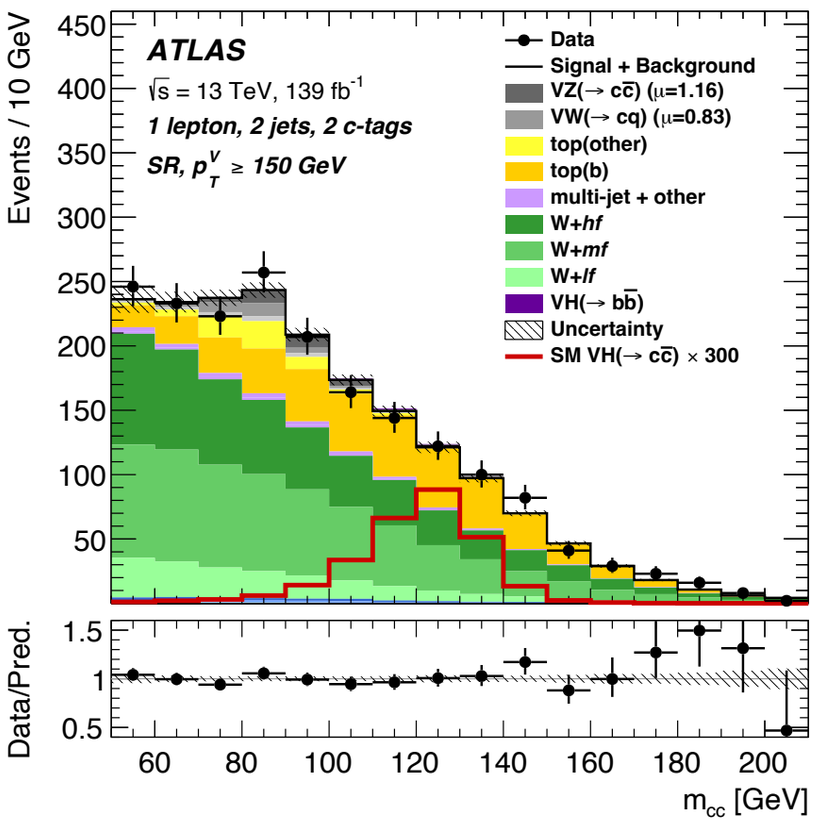

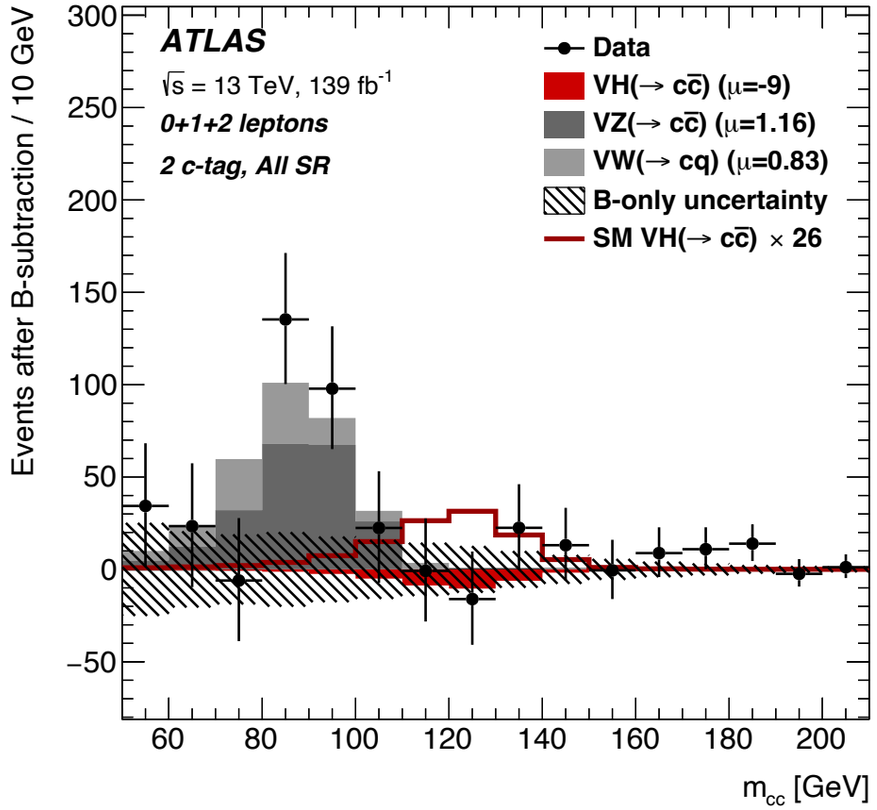

$$\mu_{VW(cq)} = 0.83 \pm 0.11\ (\text{stat.}) \pm 0.21\ (\text{syst.})$$

$$\mu_{VZ(c\bar{c})} = 1.16 \pm 0.32\ (\text{stat.}) \pm 0.36\ (\text{syst.}).$$

$$\mu_{Hc\bar{c}} < 26 \quad \left(31^{+12}_{-8}\right)$$

Combination with $VH(b\bar{b})$ $\quad |\kappa_c/\kappa_b| < 4.5$

i.e. coupling of Higgs to c is weaker than coupling to b.

EPJC 82 (2022) 717

Combined measurements

- Putting together measurements across all production & decay modes:

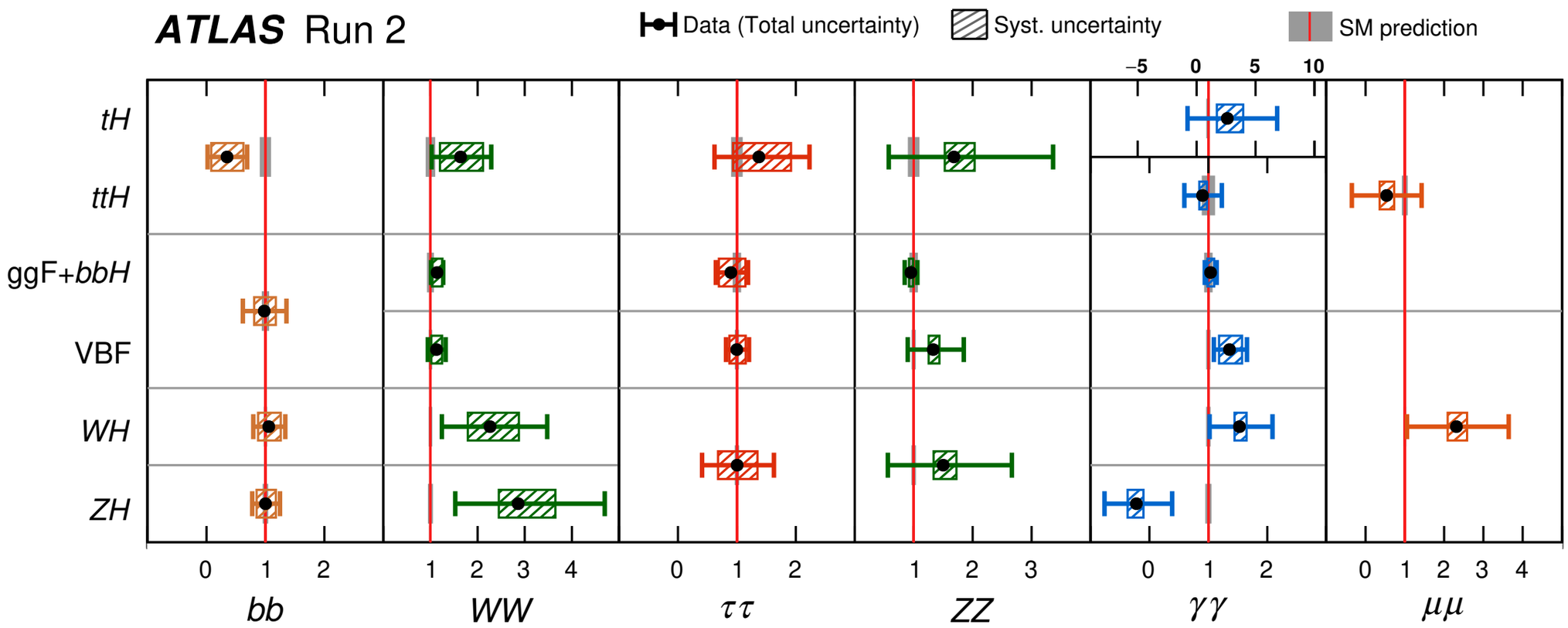

NB does not include new $VH(\rightarrow WW)$ result

Nature 607, 52-59 (2022)

Combined constraints

- Checking Higgs couplings are proportional to mass:

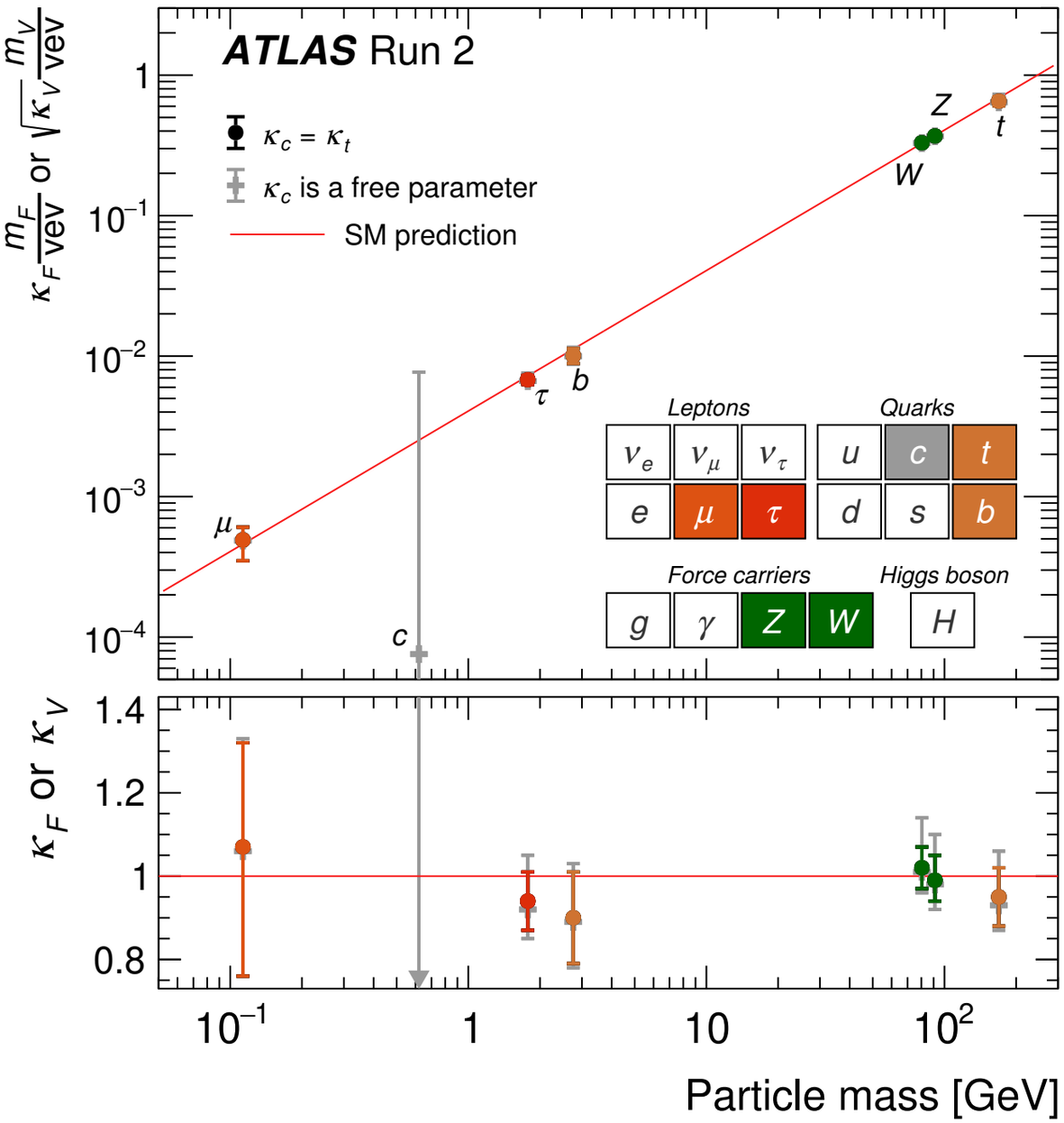

N.B. does not include new $VH(\rightarrow WW)$ result

Nature 607, 52-59 (2022)

Combined measurements

- STXS measurements combined across all channels:

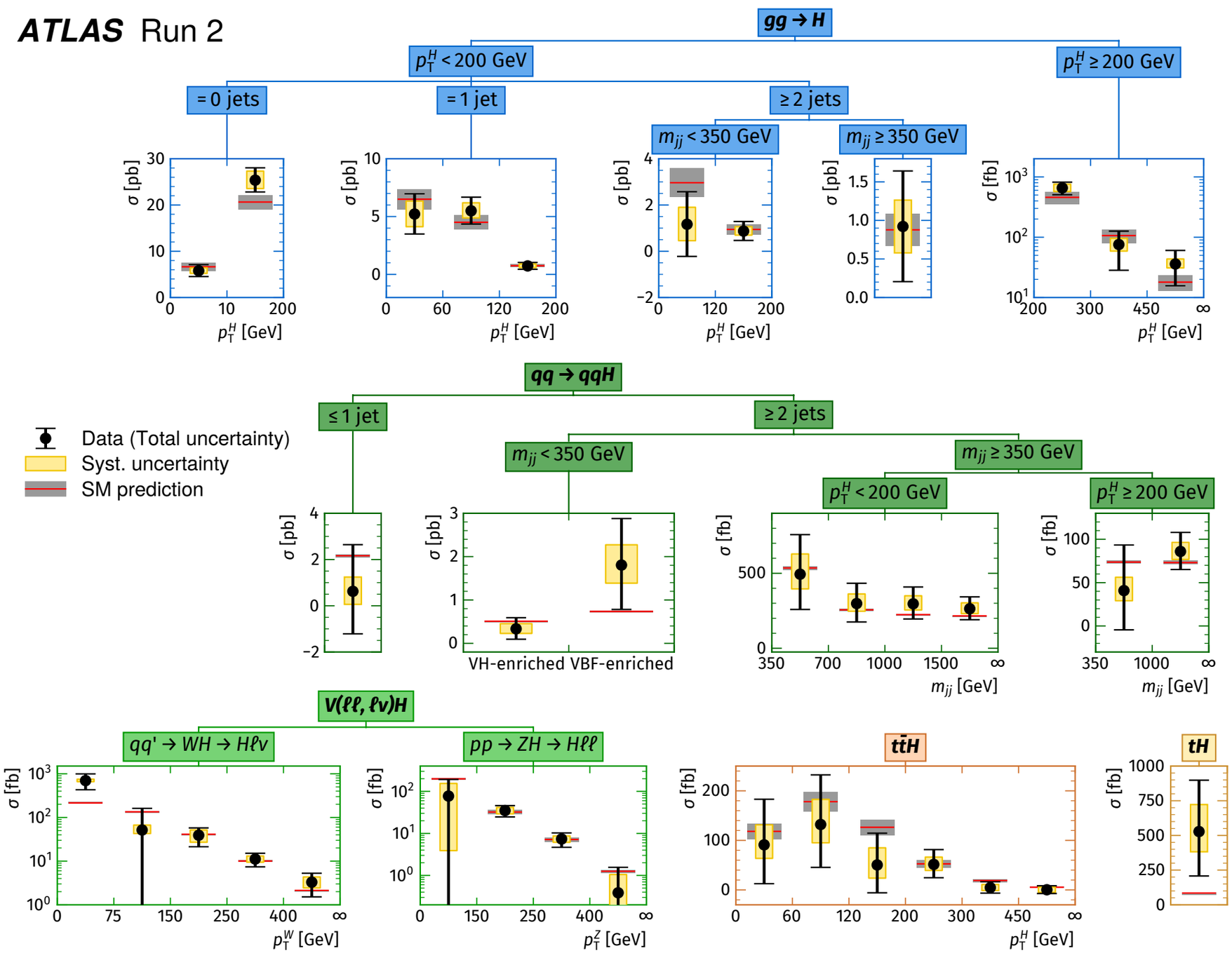

N.B. does not include new $VH(\rightarrow WW)$ result

Nature 607, 52-59 (2022)

Combined EFT constraints

- EFT allows to parameterise any high-scale new physics through effective operators:
- Recent ATLAS fit of diboson, Higgs and EWPO measurements - sensitive to ~28 (linear combinations of) operators:

$$\mathcal{L}_{\text{EFT}} = \mathcal{L}_{\text{SM}} + \sum_{i,D} \frac{C_i^D}{\Lambda^{D-4}} O_i^D ,$$

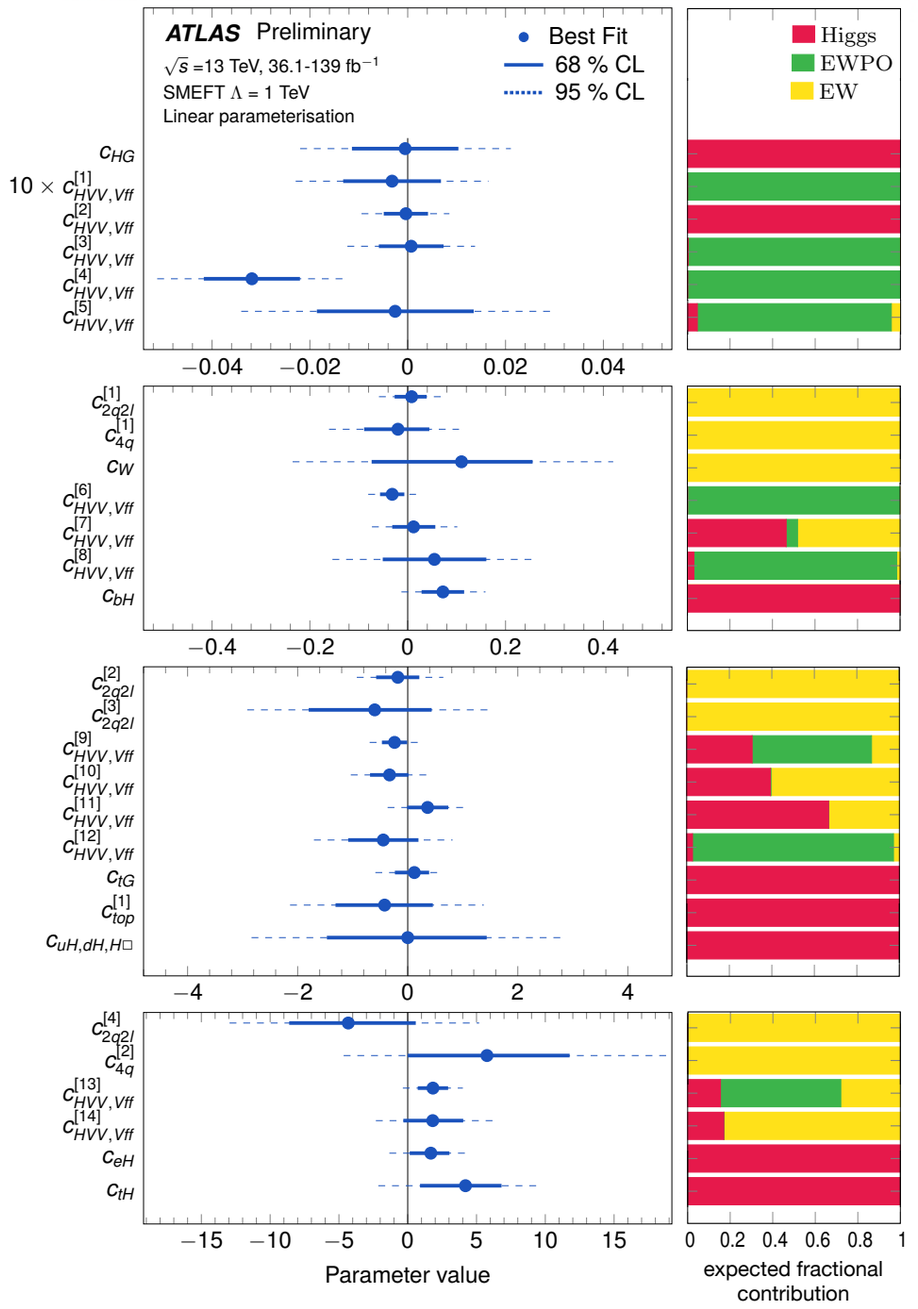

ATL-PHYS-PUB-2022-037

Combined EFT constraints

- EFT allows to parameterise any high-scale new physics through effective operators:
- Recent ATLAS fit of diboson, Higgs and EWPO measurements - sensitive to ~28 (linear combinations of) operators:

$$\mathcal{L}_{\text{EFT}} = \mathcal{L}_{\text{SM}} + \sum_{i,D} \frac{C_i^D}{\Lambda^{D-4}} O_i^D ,$$

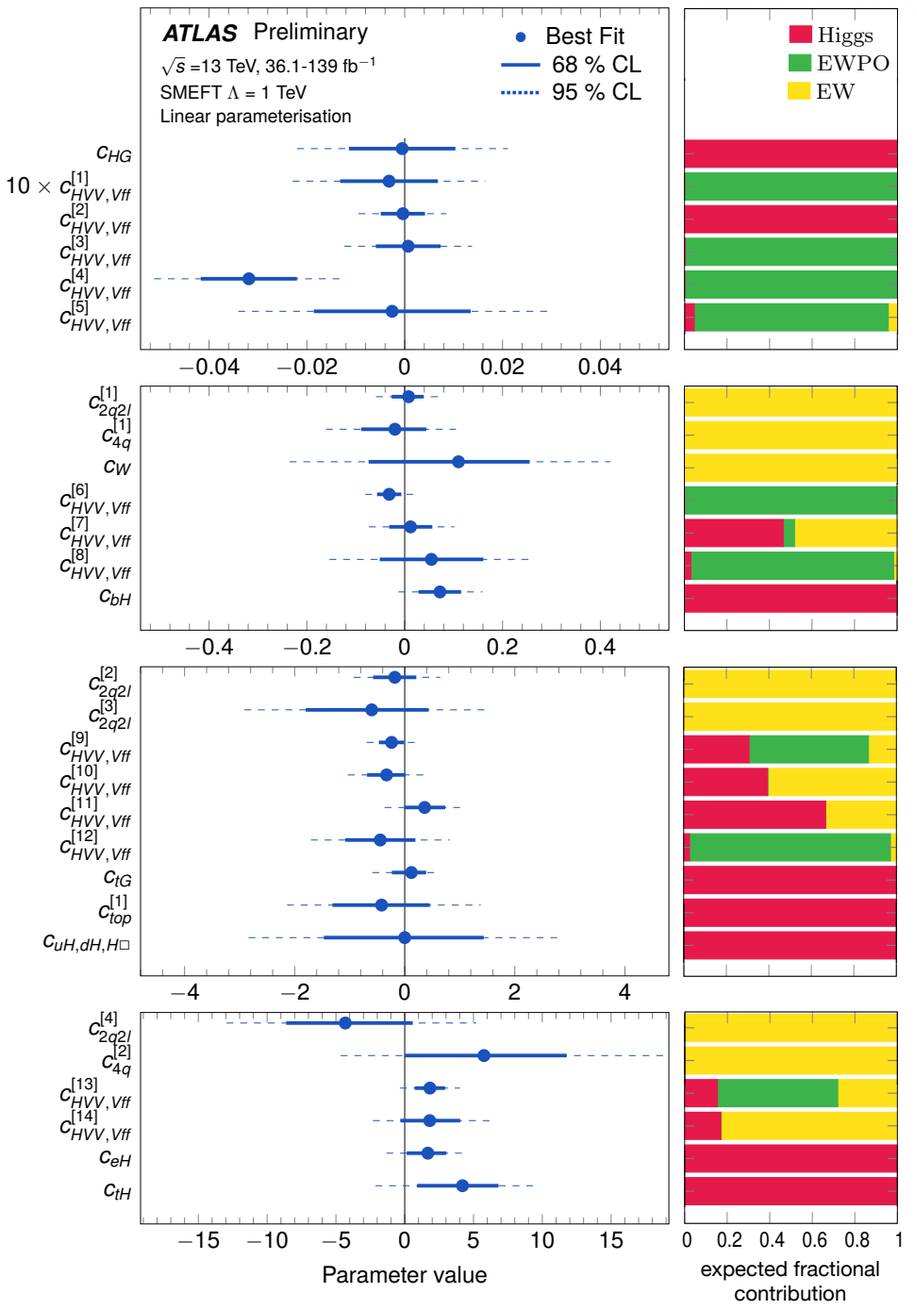

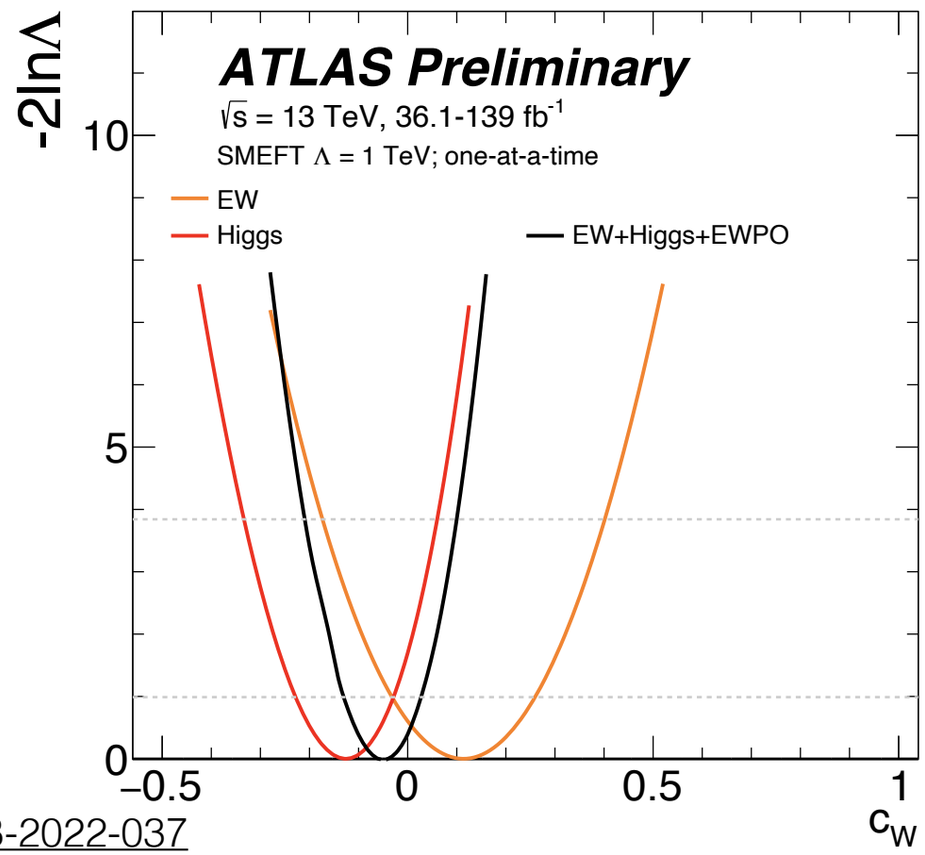

ATL-PHYS-PUB-2022-037

Conclusions

- Full run-2 statistics allows measurements of many Higgs production / decay modes.
- Discovery channels start to enter precision regime (<10% uncertainty).
- Differential measurements and small branching ratio channels still have significant statistical uncertainties.
- Looking forward to run-3 results!

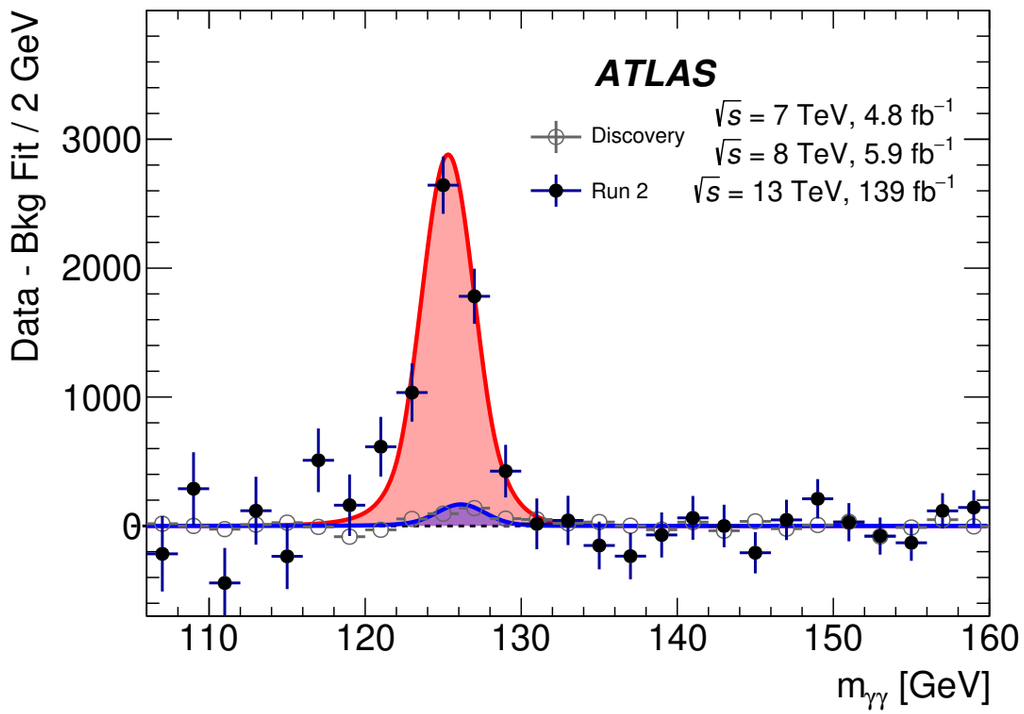

Backup

H->WW

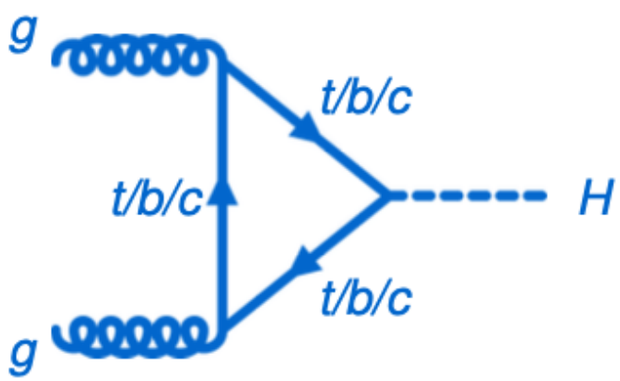

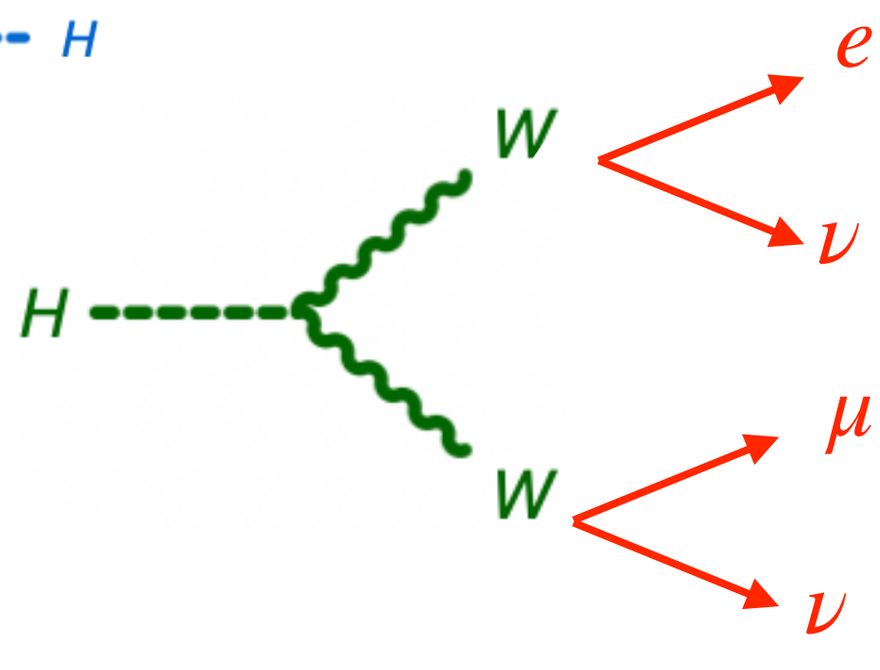

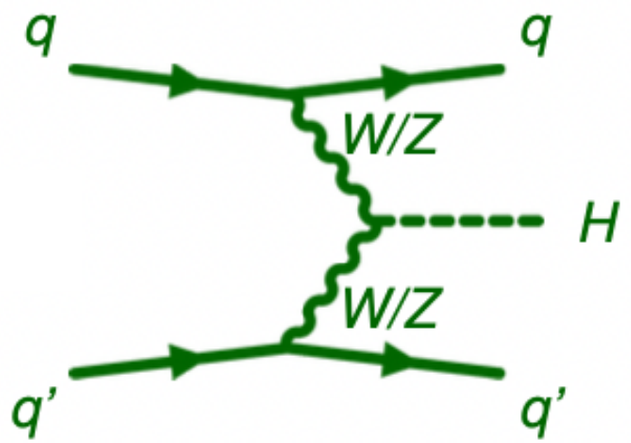

- Events categorised according to number of jets & set of selection requirements define signal regions.

- WW, $t\bar{t}$ and $Z \rightarrow \tau\tau$ backgrounds constrained in data control regions.

arXiv:2207.00338

H->WW

- Signal yields are extracted by fitting dilepton transverse mass or deep neural network (2+ jet VBF-like events).

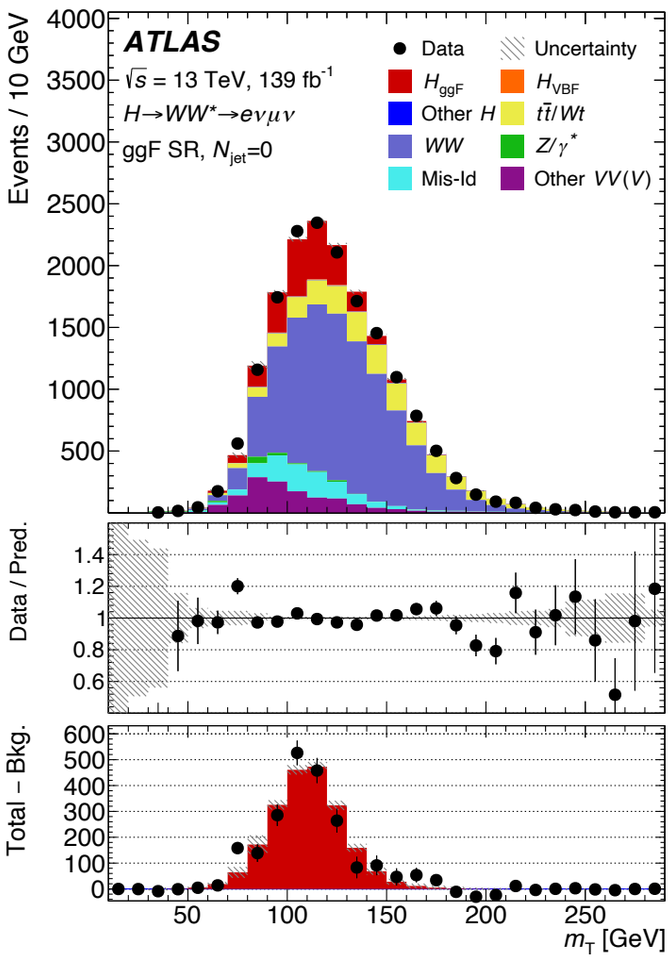

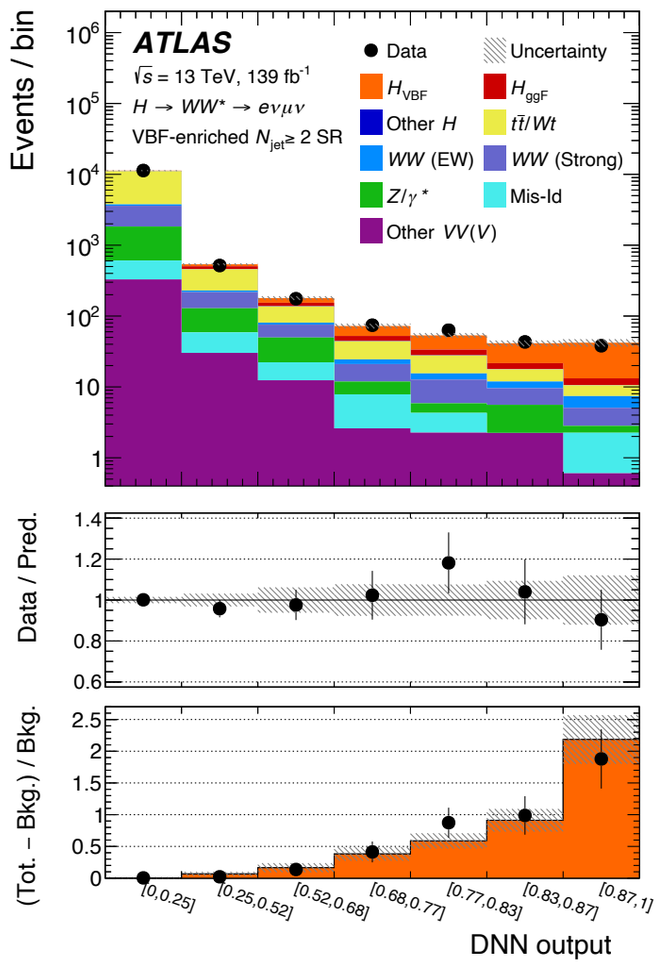

arXiv:2207.00338

H->WW

- Signal yields are extracted by fitting dilepton transverse mass or deep neural network (2+ jet VBF-like events).

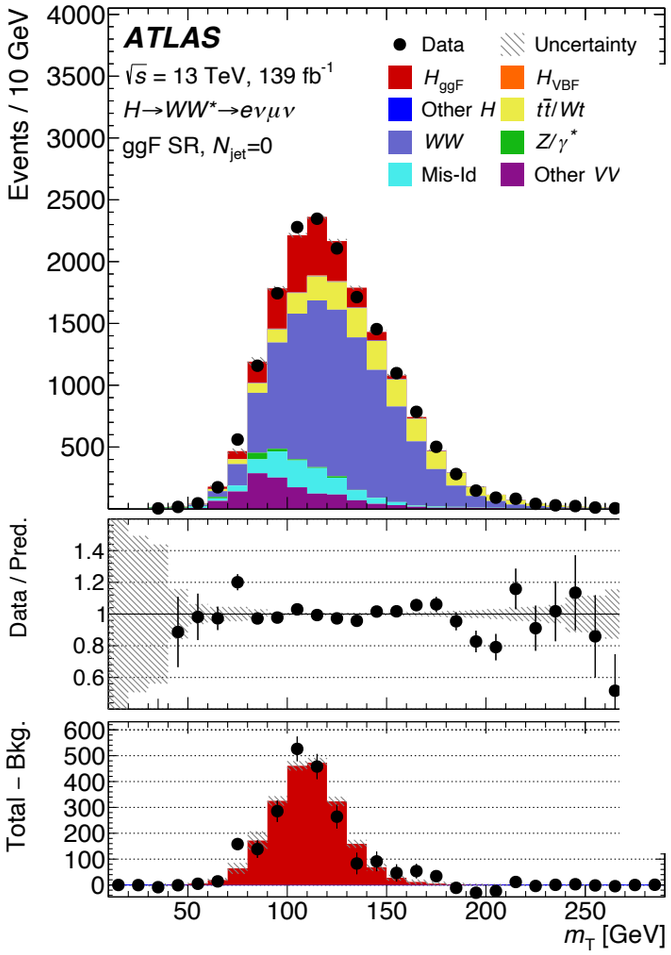

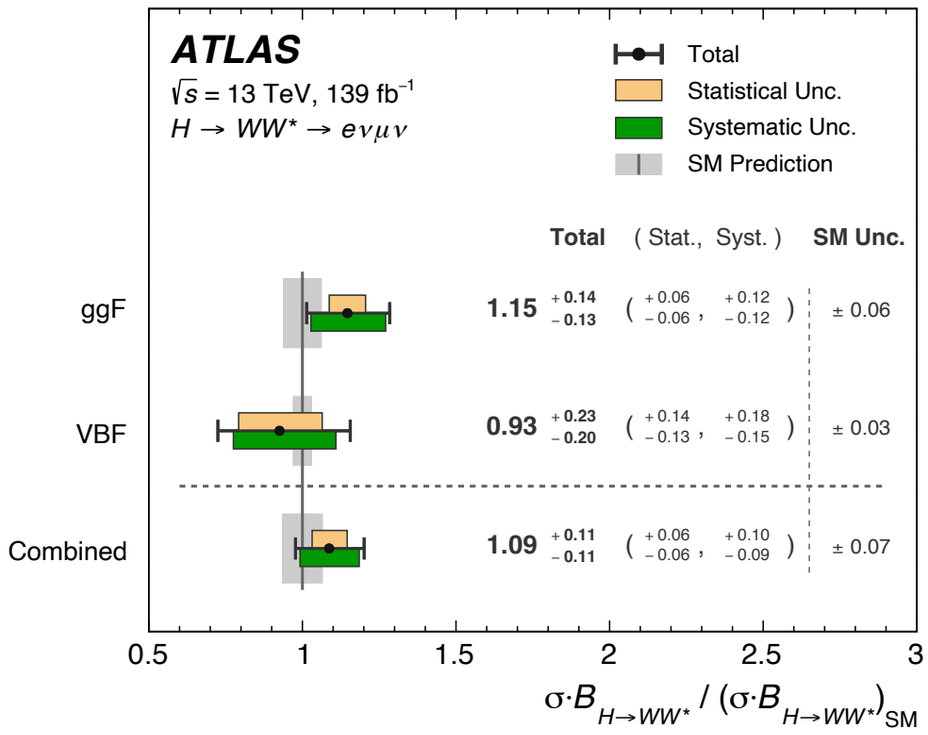

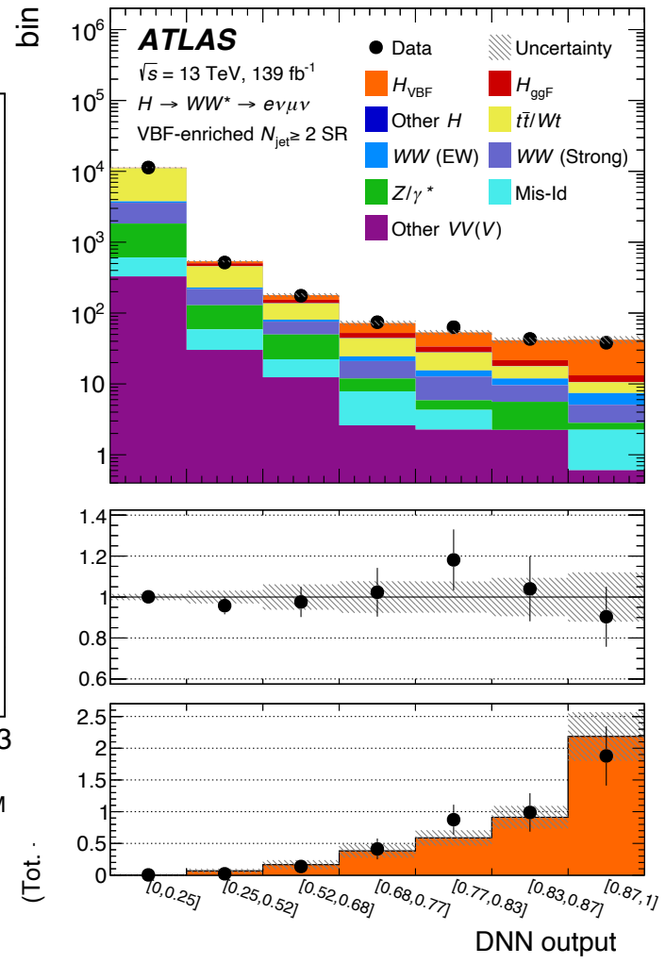

- Measurements are systematics dominated:
  - ggF: theory / experimental systematics approximately equal.
  - VBF: theory systematics dominate (additional jet modelling).

arXiv:2207.00338

H->WW

- STXS measurements in 11 bins - ggH regions split in n(jets) & Higgs p_T (p_T^H), VBF regions split by m_{jj} & p_T^H.

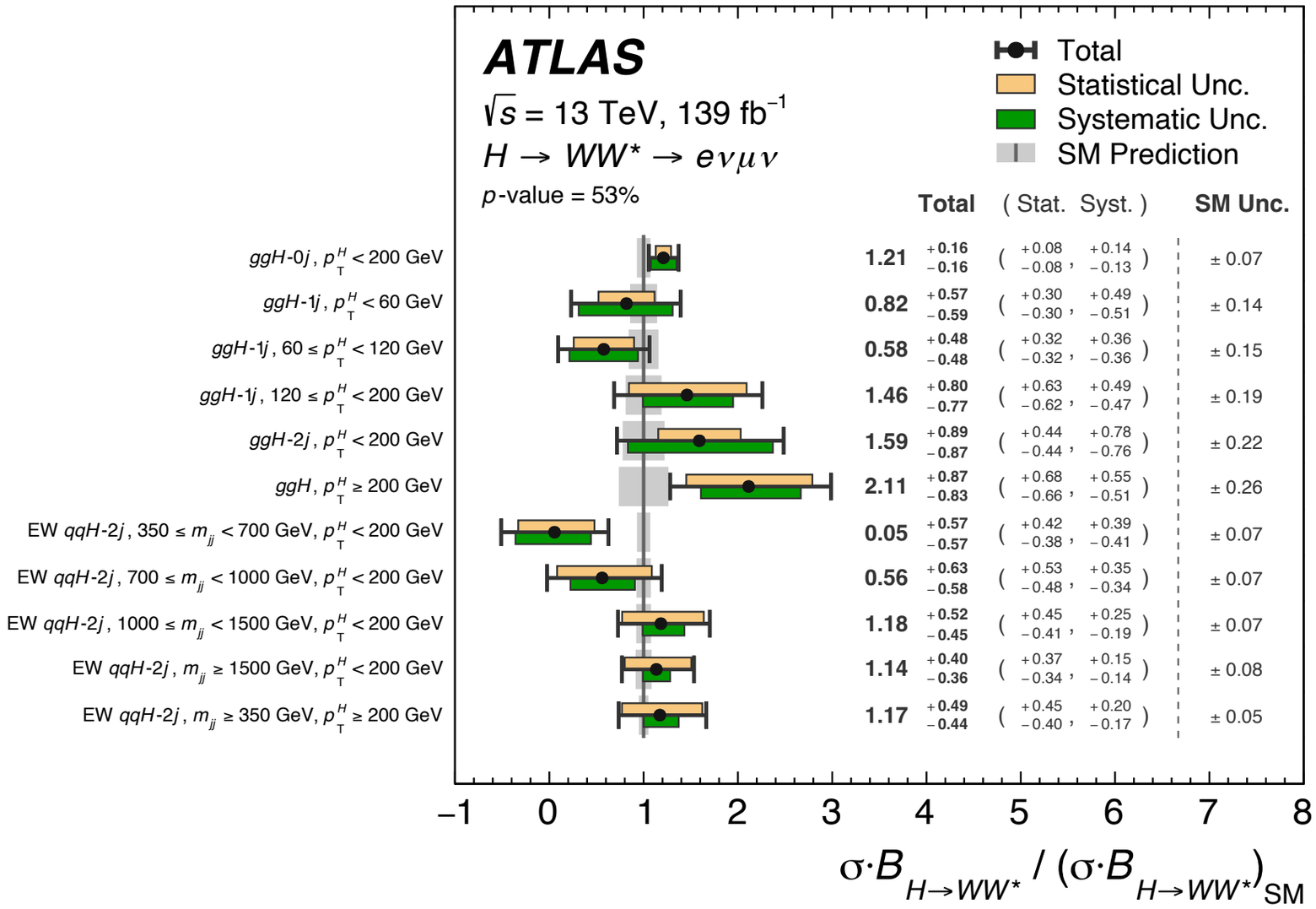

- Good agreement with SM, many bins still with significant statistical uncertainties.

arXiv:2207.00338

$H \to c\bar{c}$

- Signal regions have requirement on max $\Delta R(c, \bar{c})$:
  - $\Delta R < 1.2$ for $p_T^V > 250$ GeV, 1.6 for $150 < p_T^V < 250$ GeV, 2.3 for $p_T^V < 150$ GeV.
- V+HF jets control regions are defined by inverting the ΔR requirement and requiring $\Delta R < 2.5$.
  - Additional CR with no c or b-jets are used to constrain V+ light jets.
- Top control regions are defined by selecting 3 jet events (0, 1 lepton) or $e\mu$ events (2 lepton).

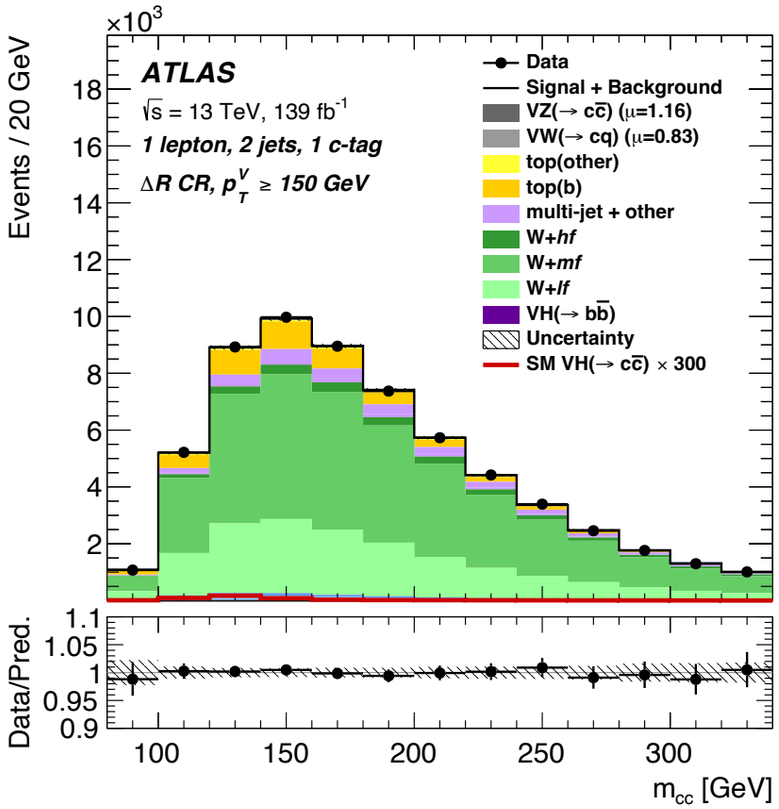

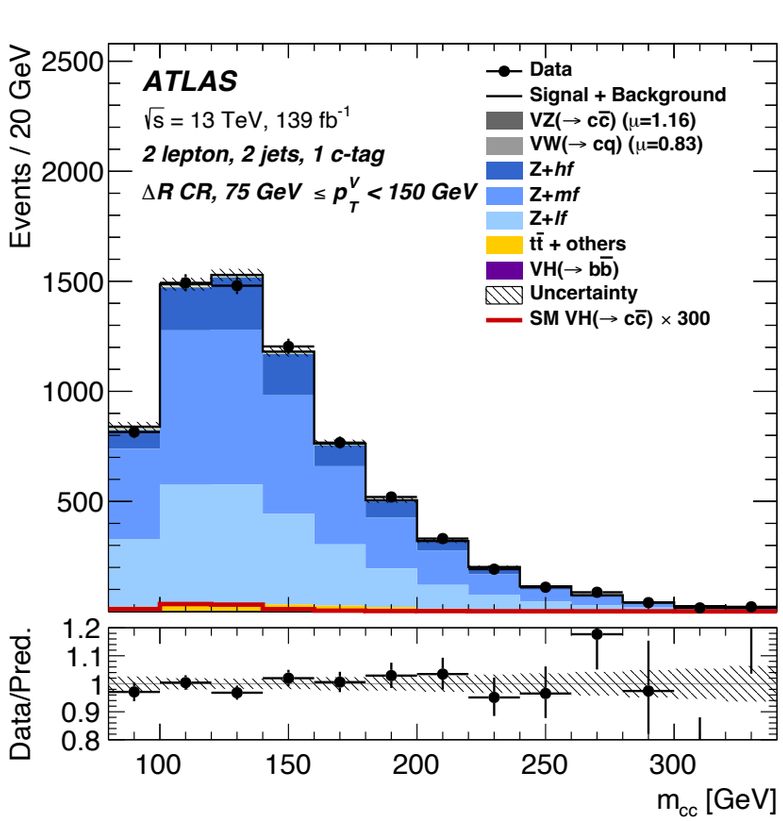

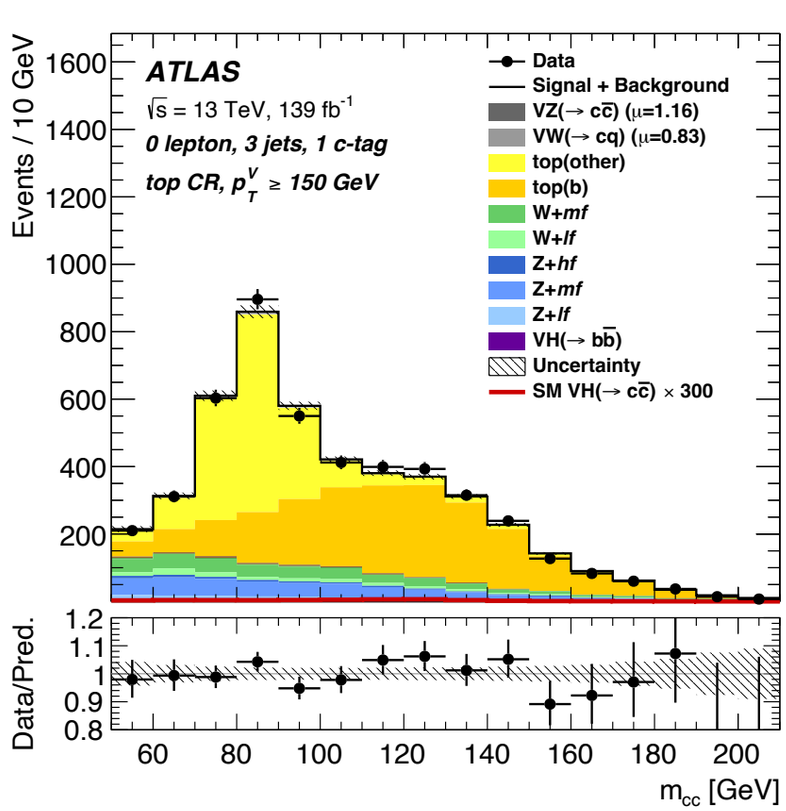

EPJC 82 (2022) 717

$H \to \gamma\gamma$

- Multi-class BDT used to build 48 STXS regions is followed by binary multivariate discriminant to separate events by purity:

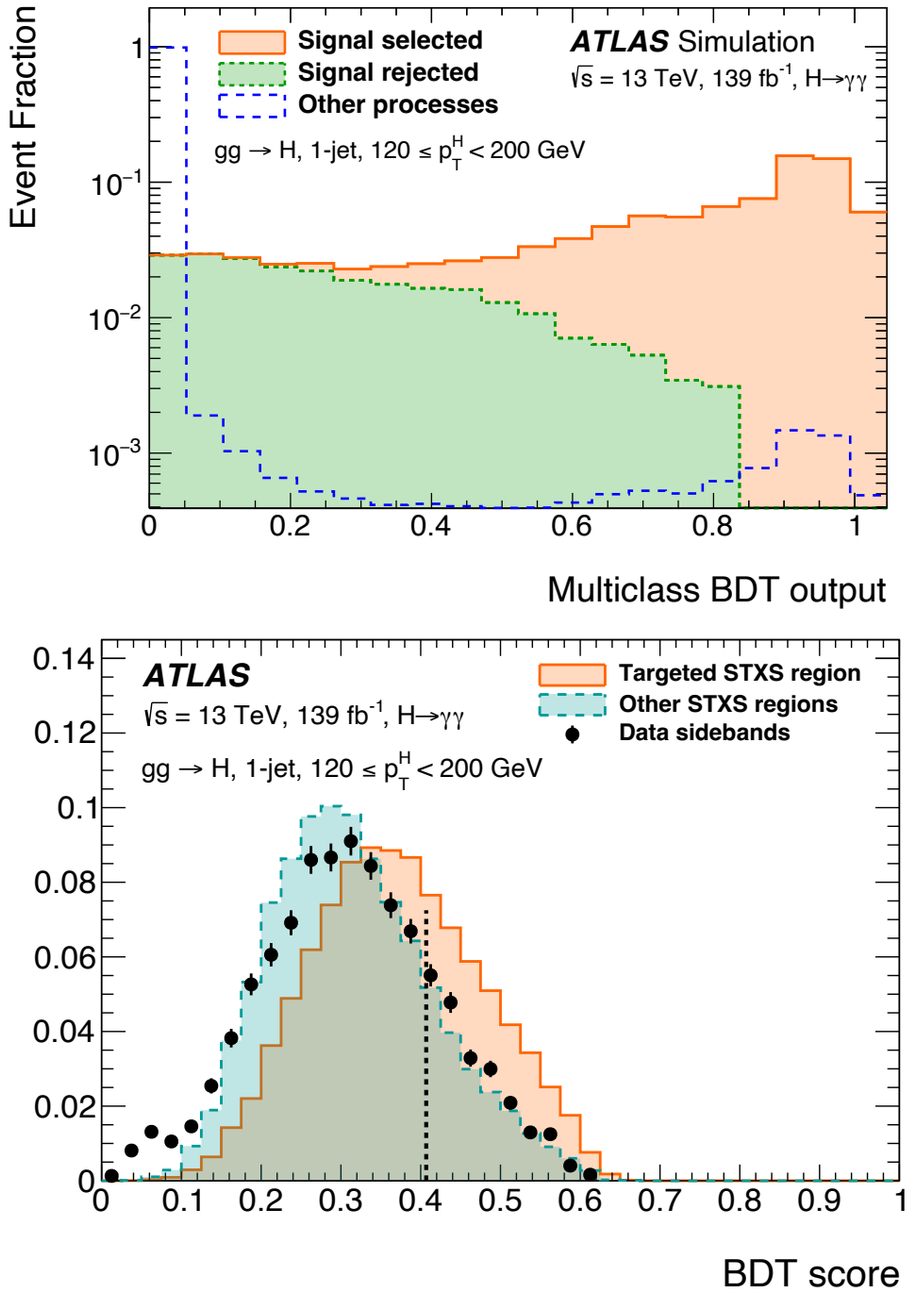

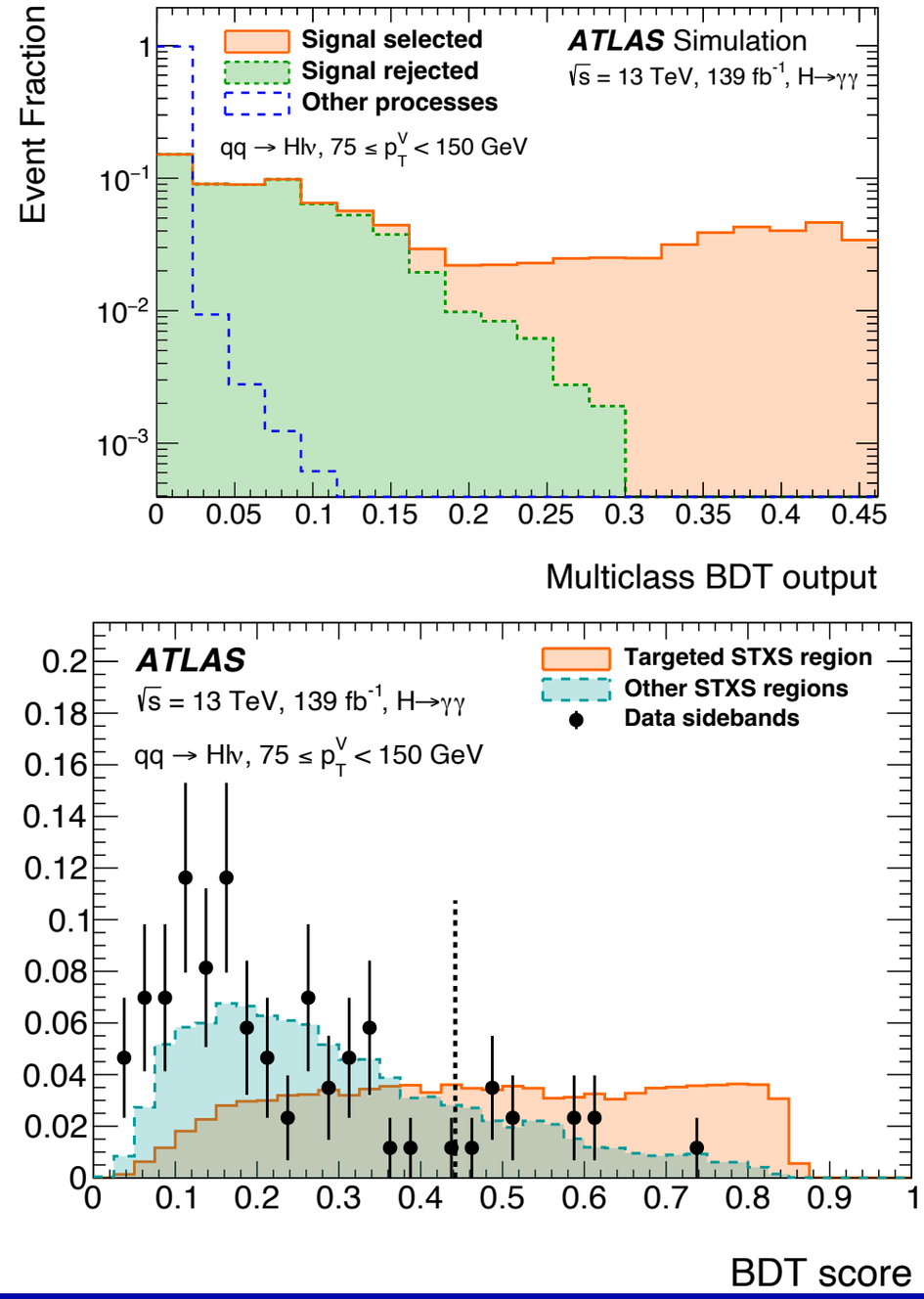

arXiv:2207.00348

$H \to \gamma\gamma$

Category	S	B	σ [GeV]	f [%]	Z
$gg \to H$					
0-jet, $p_{\mathrm{T}}^{H} < 10$ GeV	695	26 000	3.43	2.6	4.3
0-jet, $p_{\mathrm{T}}^{H} \geq 10$ GeV	1440	47 000	3.41	3.0	6.6
1-jet, $p_{\mathrm{T}}^{H} < 60$ GeV, High-purity	168	4250	3.20	3.8	2.6
1-jet, $p_{\mathrm{T}}^{H} < 60$ GeV, Med-purity	197	11 500	3.38	1.7	1.8
1-jet, $60 \leq p_{\mathrm{T}}^{H} < 120$ GeV, High-purity	186	3310	3.10	5.3	3.2
1-jet, $60 \leq p_{\mathrm{T}}^{H} < 120$ GeV, Med-purity	180	7780	3.37	2.3	2.0
1-jet, $120 \leq p_{\mathrm{T}}^{H} < 200$ GeV, High-purity	23.0	182	2.61	11	1.7
1-jet, $120 \leq p_{\mathrm{T}}^{H} < 200$ GeV, Med-purity	40.7	717	3.00	5.4	1.5
$\geq$ 2-jets, $m_{jj} < 350$ GeV, $p_{\mathrm{T}}^{H} < 60$ GeV, High-purity	23.5	1050	3.08	2.2	0.72
$\geq$ 2-jets, $m_{jj} < 350$ GeV, $p_{\mathrm{T}}^{H} < 60$ GeV, Med-purity	43.1	4360	3.39	0.98	0.65
$\geq$ 2-jets, $m_{jj} < 350$ GeV, $p_{\mathrm{T}}^{H} < 60$ GeV, Low-purity	47.5	16 800	3.51	0.28	0.37
$\geq$ 2-jets, $m_{jj} < 350$ GeV, $60 \leq p_{\mathrm{T}}^{H} < 120$ GeV, High-purity	49.1	901	3.03	5.2	1.6
$\geq$ 2-jets, $m_{jj} < 350$ GeV, $60 \leq p_{\mathrm{T}}^{H} < 120$ GeV, Med-purity	93.9	6440	3.30	1.4	1.2
$\geq$ 2-jets, $m_{jj} < 350$ GeV, $120 \leq p_{\mathrm{T}}^{H} < 200$ GeV, High-purity	15.5	74.8	2.64	17	1.7
$\geq$ 2-jets, $m_{jj} < 350$ GeV, $120 \leq p_{\mathrm{T}}^{H} < 200$ GeV, Med-purity	22.7	343	2.97	6.2	1.2
$\geq$ 2-jets, $350 \leq m_{jj} < 700$ GeV, $p_{\mathrm{T}}^{H} < 200$ GeV, High-purity	4.31	47.5	2.72	8.3	0.62
$\geq$ 2-jets, $350 \leq m_{jj} < 700$ GeV, $p_{\mathrm{T}}^{H} < 200$ GeV, Med-purity	15.4	380	3.02	3.9	0.78
$\geq$ 2-jets, $350 \leq m_{jj} < 700$ GeV, $p_{\mathrm{T}}^{H} < 200$ GeV, Low-purity	10.5	1080	3.31	0.97	0.32
$\geq$ 2-jets, $700 \leq m_{jj} < 1000$ GeV, $p_{\mathrm{T}}^{H} < 200$ GeV, High-purity	2.34	33.3	2.84	6.6	0.40
$\geq$ 2-jets, $700 \leq m_{jj} < 1000$ GeV, $p_{\mathrm{T}}^{H} < 200$ GeV, Med-purity	4.23	136	3.07	3.0	0.36
$\geq$ 2-jets, $700 \leq m_{jj} < 1000$ GeV, $p_{\mathrm{T}}^{H} < 200$ GeV, Low-purity	3.34	429	3.26	0.77	0.16
$\geq$ 2-jets, $m_{jj} \geq 1000$ GeV, $p_{\mathrm{T}}^{H} < 200$ GeV, High-purity	1.14	14.5	2.97	7.3	0.30
$\geq$ 2-jets, $m_{jj} \geq 1000$ GeV, $p_{\mathrm{T}}^{H} < 200$ GeV, Med-purity	2.52	47.5	3.10	5.0	0.36
$\geq$ 2-jets, $m_{jj} \geq 1000$ GeV, $p_{\mathrm{T}}^{H} < 200$ GeV, Low-purity	2.49	142	3.37	1.7	0.21
$200 \leq p_{\mathrm{T}}^{H} < 300$ GeV, High-purity	15.3	38.0	2.28	29	2.3
$200 \leq p_{\mathrm{T}}^{H} < 300$ GeV, Med-purity	29.4	236	2.64	11	1.9
$300 \leq p_{\mathrm{T}}^{H} < 450$ GeV, High-purity	1.52	2.13	2.02	42	0.95
$300 \leq p_{\mathrm{T}}^{H} < 450$ GeV, Med-purity	6.75	17.7	2.16	28	1.5
$300 \leq p_{\mathrm{T}}^{H} < 450$ GeV, Low-purity	4.66	43.1	2.46	9.8	0.70
$450 \leq p_{\mathrm{T}}^{H} < 650$ GeV, High-purity	1.00	1.25	1.85	45	0.81
$450 \leq p_{\mathrm{T}}^{H} < 650$ GeV, Med-purity	0.800	2.00	1.98	29	0.53
$450 \leq p_{\mathrm{T}}^{H} < 650$ GeV, Low-purity	0.830	10.7	2.19	7.2	0.25
$p_{\mathrm{T}}^{H} \geq 650$ GeV	0.220	1.08	1.73	17	0.20
$qq' \to Hqq'$					
0-jet, High-purity	0.330	25.0	3.33	1.3	0.07
0-jet, Med-purity	1.27	471	3.35	0.27	0.06
0-jet, Low-purity	10.7	18 800	3.48	0.06	0.08
1-jet, High-purity	1.08	2.78	2.99	28	0.61
1-jet, Med-purity	3.50	26.1	3.11	12	0.67
1-jet, Low-purity	2.88	145	3.24	2.0	0.24
$\geq$ 2-jets, $m_{jj} < 60$ GeV, High-purity	0.350	2.10	2.71	14	0.24
$\geq$ 2-jets, $m_{jj} < 60$ GeV, Med-purity	0.670	19.0	2.79	3.4	0.15
$\geq$ 2-jets, $m_{jj} < 60$ GeV, Low-purity	1.92	243	2.93	0.78	0.12
$\geq$ 2-jets, $60 \leq m_{jj} < 120$ GeV, High-purity	3.45	6.34	2.65	35	1.3
$\geq$ 2-jets, $60 \leq m_{jj} < 120$ GeV, Med-purity	4.99	43.0	2.85	10	0.75
$\geq$ 2-jets, $60 \leq m_{jj} < 120$ GeV, Low-purity	2.99	87.3	3.01	3.3	0.32
$\geq$ 2-jets, $120 \leq m_{jj} < 350$ GeV, High-purity	2.98	24.4	2.93	11	0.59
$\geq$ 2-jets, $120 \leq m_{jj} < 350$ GeV, Med-purity	6.73	204	2.94	3.2	0.47
$\geq$ 2-jets, $120 \leq m_{jj} < 350$ GeV, Low-purity	8.78	1360	2.99	0.64	0.24
$\geq$ 2-jets, $350 \leq m_{jj} < 700$ GeV, $p_{\mathrm{T}}^{H} < 200$ GeV, High-purity	2.52	2.75	2.96	48	1.4
$\geq$ 2-jets, $350 \leq m_{jj} < 700$ GeV, $p_{\mathrm{T}}^{H} < 200$ GeV, Med-purity	9.15	34.7	3.06	21	1.5
$\geq$ 2-jets, $350 \leq m_{jj} < 700$ GeV, $p_{\mathrm{T}}^{H} < 200$ GeV, Low-purity	5.97	106	3.27	5.3	0.57
$\geq$ 2-jets, $700 \leq m_{jj} < 1000$ GeV, $p_{\mathrm{T}}^{H} < 200$ GeV, High-purity	2.91	3.00	2.90	49	1.5
$\geq$ 2-jets, $700 \leq m_{jj} < 1000$ GeV, $p_{\mathrm{T}}^{H} < 200$ GeV, Med-purity	5.60	22.7	3.11	20	1.1
$\geq$ 2-jets, $m_{jj} \geq 1000$ GeV, $p_{\mathrm{T}}^{H} < 200$ GeV, High-purity	10.8	3.89	3.01	74	4.2
$\geq$ 2-jets, $m_{jj} \geq 1000$ GeV, $p_{\mathrm{T}}^{H} < 200$ GeV, Med-purity	10.7	19.0	3.23	36	2.3
$\geq$ 2-jets, $m_{jj} \geq 1000$ GeV, $p_{\mathrm{T}}^{H} < 200$ GeV, Low-purity	1.31	2.19	2.48	37	0.81
$\geq$ 2-jets, $350 \leq m_{jj} < 700$ GeV, $p_{\mathrm{T}}^{H} \geq 200$ GeV, Med-purity	1.40	9.22	2.49	13	0.45
$\geq$ 2-jets, $350 \leq m_{jj} < 700$ GeV, $p_{\mathrm{T}}^{H} \geq 200$ GeV, Low-purity	1.16	65.5	2.54	1.7	0.14
$\geq$ 2-jets, $700 \leq m_{jj} < 1000$ GeV, $p_{\mathrm{T}}^{H} \geq 200$ GeV, High-purity	2.51	3.02	2.43	45	1.3
$\geq$ 2-jets, $700 \leq m_{jj} < 1000$ GeV, $p_{\mathrm{T}}^{H} \geq 200$ GeV, Med-purity	1.49	47.4	2.54	3.0	0.22
$\geq$ 2-jets, $m_{jj} \geq 1000$ GeV, $p_{\mathrm{T}}^{H} \geq 200$ GeV, High-purity	5.65	1.57	2.39	78	3.3
$\geq$ 2-jets, $m_{jj} \geq 1000$ GeV, $p_{\mathrm{T}}^{H} \geq 200$ GeV, Med-purity	2.96	6.31	2.55	32	1.1
$qq \to H\ell\nu$					
$p_{\mathrm{T}}^{V} < 75$ GeV, High-purity	1.91	4.91	3.17	28	0.81
$p_{\mathrm{T}}^{V} < 75$ GeV, Med-purity	2.59	20.2	3.28	11	0.57
$75 \leq p_{\mathrm{T}}^{V} < 150$ GeV, High-purity	2.62	2.05	3.02	56	1.6
$75 \leq p_{\mathrm{T}}^{V} < 150$ GeV, Med-purity	2.08	12.4	3.23	14	0.58
$150 \leq p_{\mathrm{T}}^{V} < 250$ GeV, High-purity	1.74	2.06	2.78	46	1.1
$150 \leq p_{\mathrm{T}}^{V} < 250$ GeV, Med-purity	0.16	2.90	3.17	5.2	0.09
$p_{\mathrm{T}}^{V} \geq 250$ GeV, High-purity	1.36	1.79	2.41	43	0.91
$p_{\mathrm{T}}^{V} \geq 250$ GeV, Med-purity	0.02	3.12	3.15	0.78	0.01
$pp \to H\ell\ell$					
$p_{\mathrm{T}}^{V} < 75$ GeV, High-purity	1.14	1.82	3.25	39	0.78
$p_{\mathrm{T}}^{V} < 75$ GeV, Med-purity	1.06	215	3.29	0.49	0.07
$75 \leq p_{\mathrm{T}}^{V} < 150$ GeV, High-purity	1.07	1.58	3.08	40	0.77
$75 \leq p_{\mathrm{T}}^{V} < 150$ GeV, Med-purity	0.02	1.81	3.06	1.2	0.02
$150 \leq p_{\mathrm{T}}^{V} < 250$ GeV, High-purity	0.71	1.79	2.78	28	0.50
$150 \leq p_{\mathrm{T}}^{V} < 250$ GeV, Med-purity	0.10	16.5	2.88	0.62	0.03
$p_{\mathrm{T}}^{V} \geq 250$ GeV	0.27	2.06	2.48	12	0.18
$pp \to H\nu\bar{\nu}$					
$p_{\mathrm{T}}^{V} < 75$ GeV, High-purity	0.60	170	3.50	0.35	0.05
$p_{\mathrm{T}}^{V} < 75$ GeV, Med-purity	1.15	1020	3.57	0.11	0.04
$p_{\mathrm{T}}^{V} < 75$ GeV, Low-purity	0.87	2630	3.67	0.03	0.02
$75 \leq p_{\mathrm{T}}^{V} < 150$ GeV, High-purity	0.58	2.30	2.97	20	0.37
$75 \leq p_{\mathrm{T}}^{V} < 150$ GeV, Med-purity	1.83	17.8	3.26	9.3	0.43
$75 \leq p_{\mathrm{T}}^{V} < 150$ GeV, Low-purity	2.18	288	3.44	0.75	0.13
$150 \leq p_{\mathrm{T}}^{V} < 250$ GeV, High-purity	0.92	2.00	2.75	32	0.61
$150 \leq p_{\mathrm{T}}^{V} < 250$ GeV, Med-purity	0.75	2.54	2.94	23	0.45
$150 \leq p_{\mathrm{T}}^{V} < 250$ GeV, Low-purity	0.26	11.7	3.28	2.2	0.08
$p_{\mathrm{T}}^{V} \geq 250$ GeV, High-purity	0.67	1.55	2.46	30	0.50
$p_{\mathrm{T}}^{V} \geq 250$ GeV, Med-purity	0.05	1.97	3.05	2.6	0.04
$t\bar{t}H$					
$p_{\mathrm{T}}^{H} < 60$ GeV, High-purity	3.04	4.01	3.18	43	1.4
$p_{\mathrm{T}}^{H} < 60$ GeV, Med-purity	2.78	13.3	3.37	17	0.74
$60 \leq p_{\mathrm{T}}^{H} < 120$ GeV, High-purity	4.30	4.09	3.06	51	1.9
$60 \leq p_{\mathrm{T}}^{H} < 120$ GeV, Med-purity	2.99	8.61	3.31	26	0.97
$120 \leq p_{\mathrm{T}}^{H} < 200$ GeV, High-purity	4.65	3.52	2.73	57	2.1
$120 \leq p_{\mathrm{T}}^{H} < 200$ GeV, Med-purity	1.66	4.16	2.93	29	0.77
$200 \leq p_{\mathrm{T}}^{H} < 300$ GeV	3.39	2.26	2.46	60	1.9
$p_{\mathrm{T}}^{H} \geq 300$ GeV	2.73	1.66	2.12	62	1.8
tH					
$tHqb$, High-purity	0.55	2.16	3.04	20	0.36
$tHqb$, Med-purity	0.14	2.78	3.45	4.9	0.09
$tHqb$, BSM ($\kappa_t = -1$)	0.12	1.86	3.25	6.0	0.09
tHW	0.16	6.91	2.74	2.3	0.06
Low-purity top	5.18	65.8	3.32	7.3	0.63

arXiv:2207.00348

$H \to \gamma\gamma$

- Systematic uncertainties on cross-section measurements:

	ggF + $b\bar{b}$H	VBF	WH	ZH	$t\bar{t}H$	tH
Uncertainty source	$\Delta\sigma$[%]	$\Delta\sigma$[%]	$\Delta\sigma$[%]	$\Delta\sigma$[%]	$\Delta\sigma$[%]	$\Delta\sigma$[%]
Theory uncertainties						
Higher-order QCD terms	±1.4	±4.1	±4.1	±12	±2.8	±16
Underlying event and parton shower	±2.5	±16	±2.5	±4.0	±3.6	±48
PDF and α_s	< ±1	±2.0	±1.4	±2.3	< ±1	±5.8
Matrix element	< ±1	±3.2	< ±1	±1.2	±2.5	±8.2
Heavy-flavour jet modelling in non-$t\bar{t}H$ processes	< ±1	< ±1	< ±1	< ±1	< ±1	±13
Experimental uncertainties						
Photon energy resolution	±3.0	±3.0	±3.8	±4.8	±3.0	±12
Photon efficiency	±2.7	±2.7	±3.3	±3.6	±2.9	±9.3
Luminosity	±1.8	±2.0	±2.4	±2.7	±2.2	±6.6
Pile-up	±1.4	±2.2	±2.0	±2.3	±1.4	±7.3
Background modelling	±2.0	±4.6	±3.6	±7.2	±2.5	±63
Photon energy scale	< ±1	< ±1	< ±1	±1.3	< ±1	±5.6
Jet/$E_{\mathrm{T}}^{\mathrm{miss}}$	< ±1	±6.8	< ±1	±2.2	±3.5	±22
Flavour tagging	< ±1	< ±1	< ±1	< ±1	±1.5	±3.4
Leptons	< ±1	< ±1	< ±1	< ±1	< ±1	±1.8
Higgs boson mass	< ±1	< ±1	< ±1	< ±1	< ±1	< ±1

arXiv:2207.00348

$H \to \gamma\gamma$ Kappa

- Allow for different physics in production (κ_g) and decay (κ_γ):

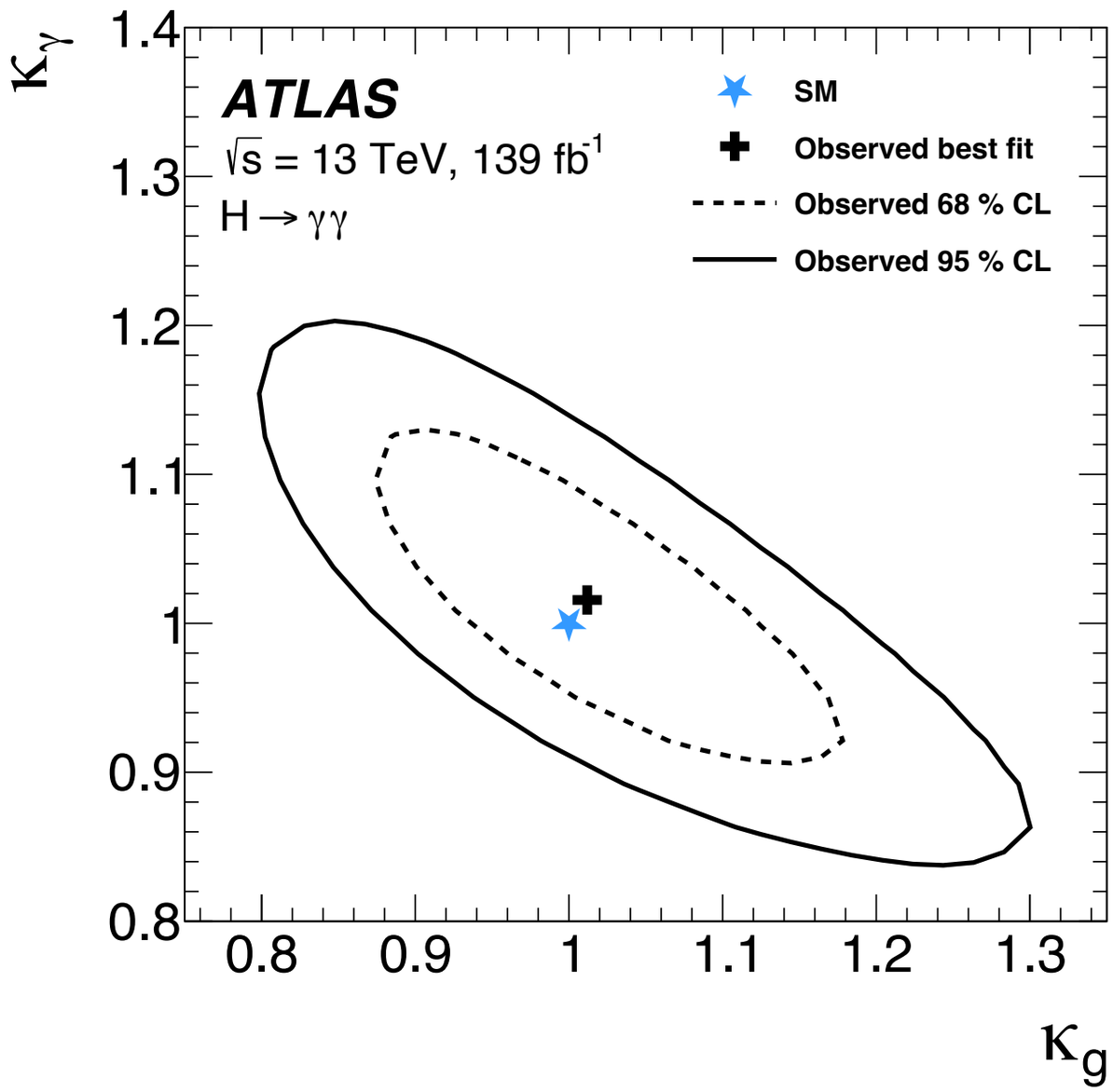

arXiv:2207.00348

$VH; H \rightarrow WW$

- Control regions & background strategy:

Channel	Normalised in the fit	Control Region	Data-driven
Opposite-sign 2ℓ	–	$t\bar{t}/Wt$, Z+jets, WW	$W+\gamma$, W+jets
Same-sign 2ℓ	$W(Z/\gamma^*)$	–	$V+\gamma$, V+jets
3ℓ	WWW	$W(Z/\gamma^*)$	$Z+\gamma$, Z+jets, $t\bar{t}/Wt$, WW+jets
4ℓ	–	ZZ	$W(Z/\gamma^*)$+jets, $t\bar{t}W/tZ$, Z+jets, $t\bar{t}/Wt$

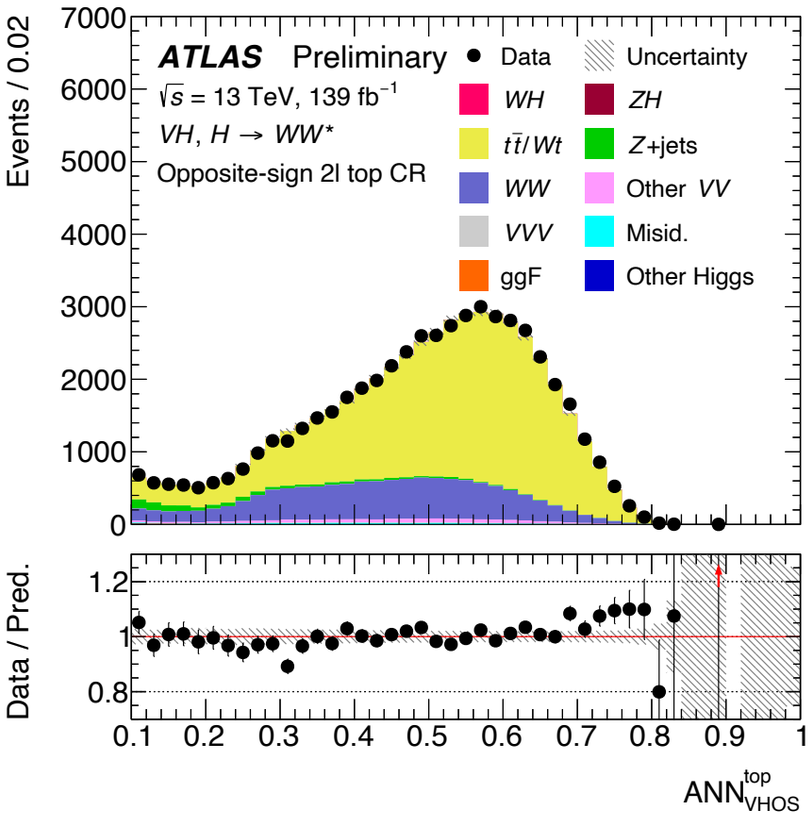

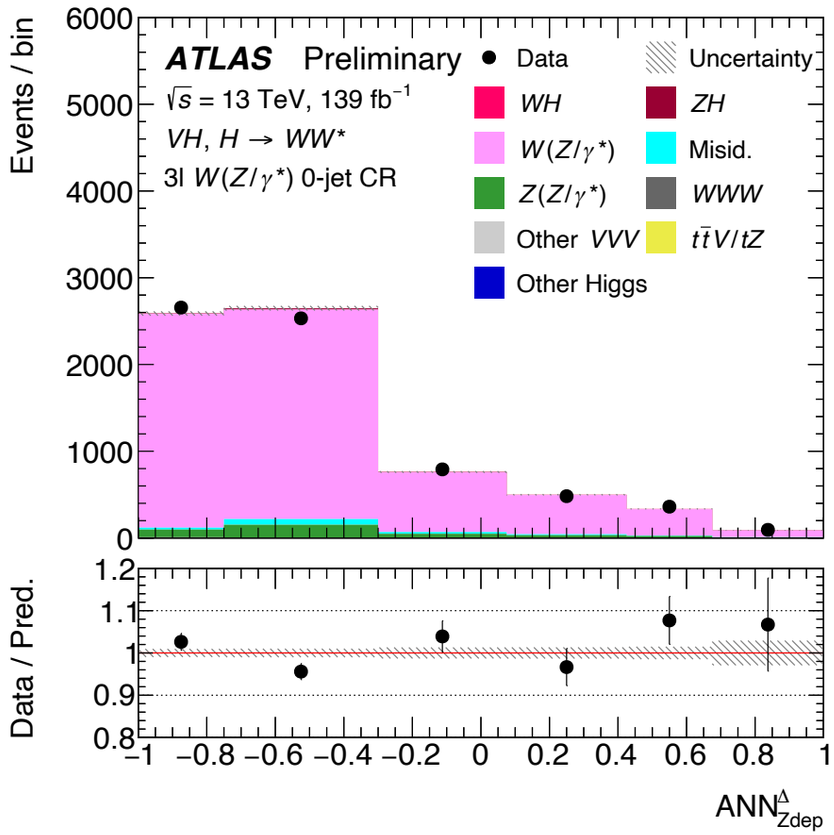

ATLAS-CONF-2022-067

$H \to \mu\mu$

- Events with two muons (p_T > 27, 15 GeV) are split into 20 categories defined by cuts & BDTs.
  - Categories are related to the Higgs production mode (ttH, VH, VBF, gluon-fusion).
- Simultaneous fit to $m_{\mu\mu}$ distribution in all 20 categories:

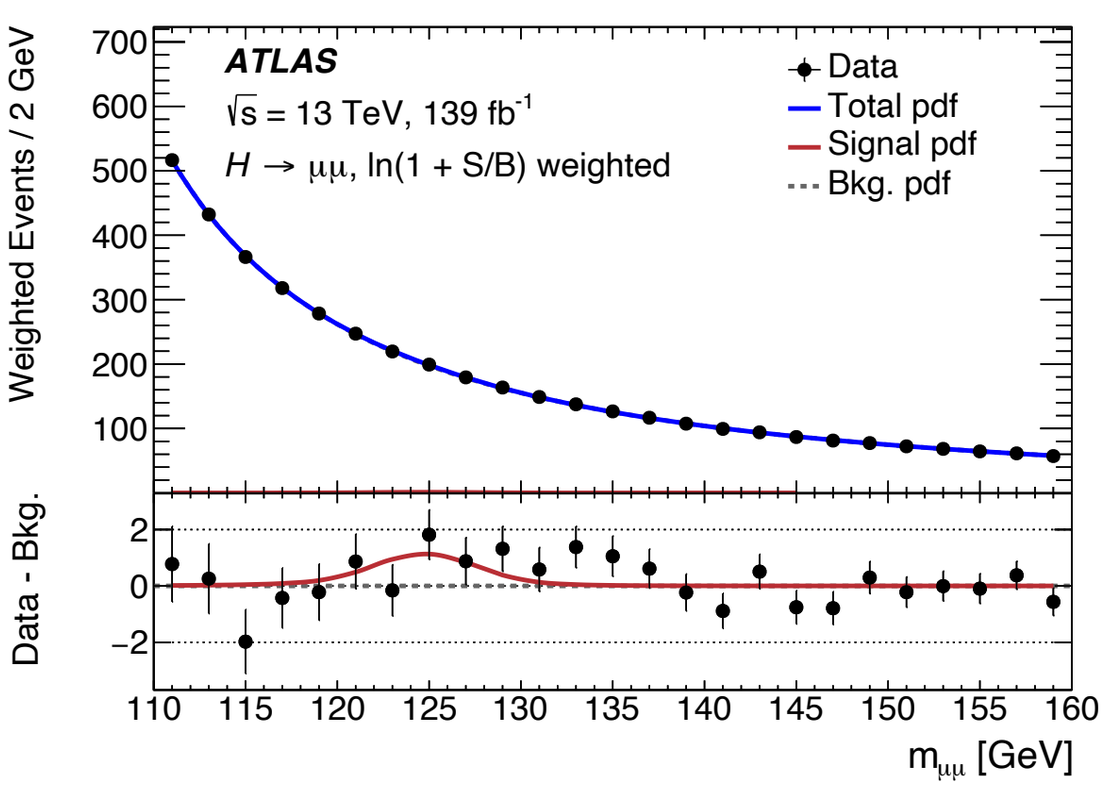

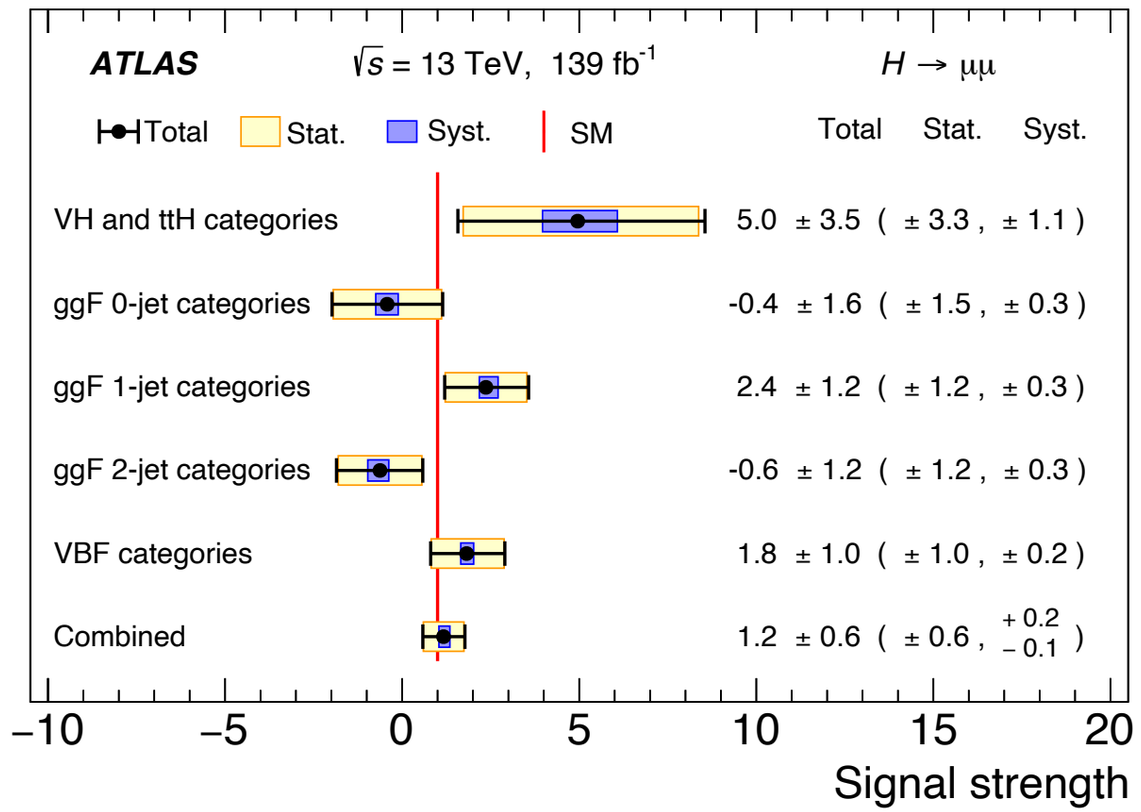

$H \to \tau\tau$

- Taus decay before the detector - identify via leptonic ($\tau_{e/\mu}\tau_{\text{lep}}$) and hadronic ($\tau_{\text{had}}$) decays in combinations $\tau_e\tau_\mu$, $\tau_{\text{lep}}\tau_{\text{had}}$, $\tau_{\text{had}}\tau_{\text{had}}$.
- Events are split into 12 categories related to the STXS categories:

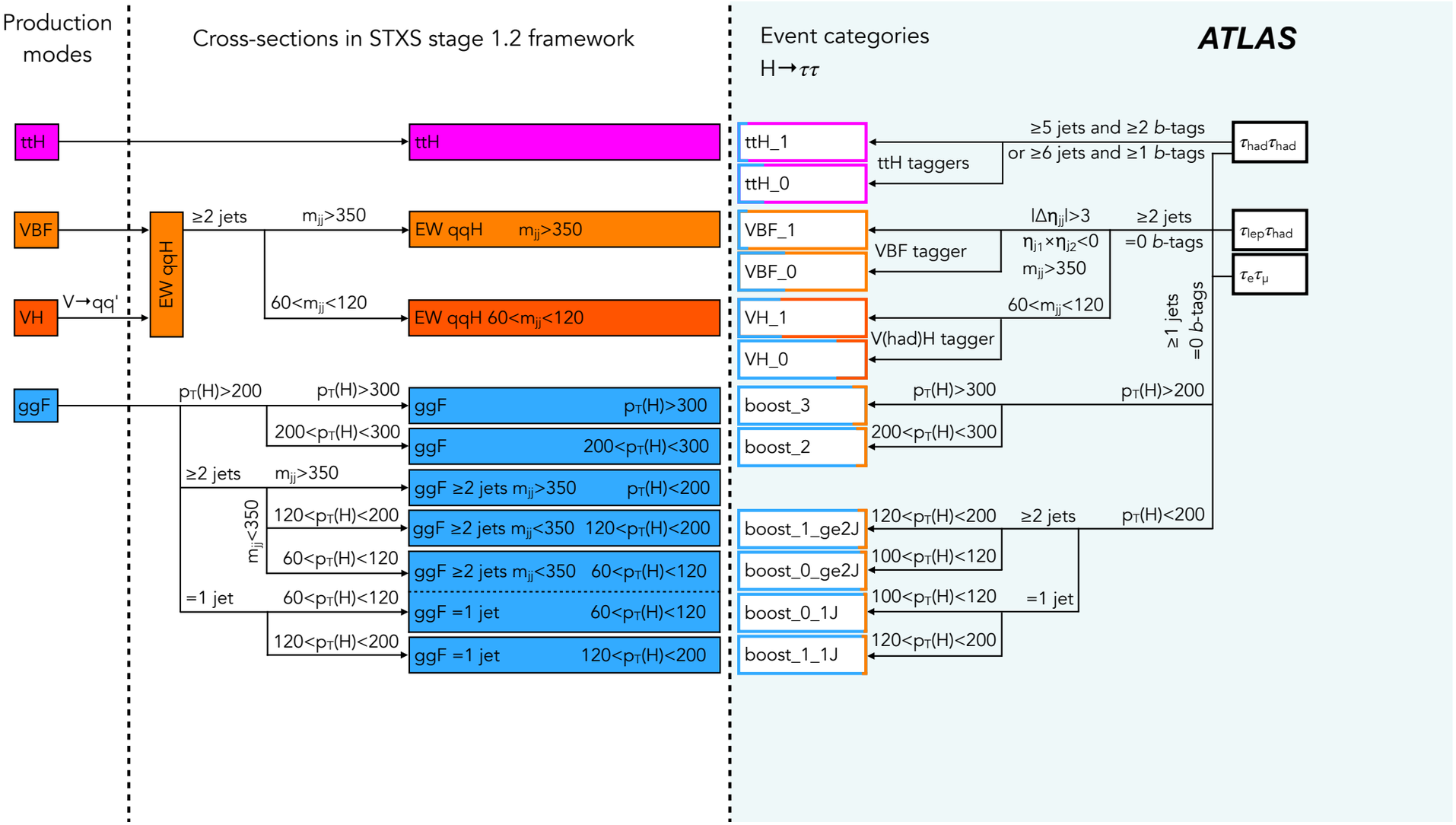

JHEP 08 (2022) 175

$H \to \tau\tau$

- Events are split into 12 categories related to the STXS categories.
- Important $Z \to \tau\tau$ background controlled by reweighting $Z \to ee/\mu\mu$ events:

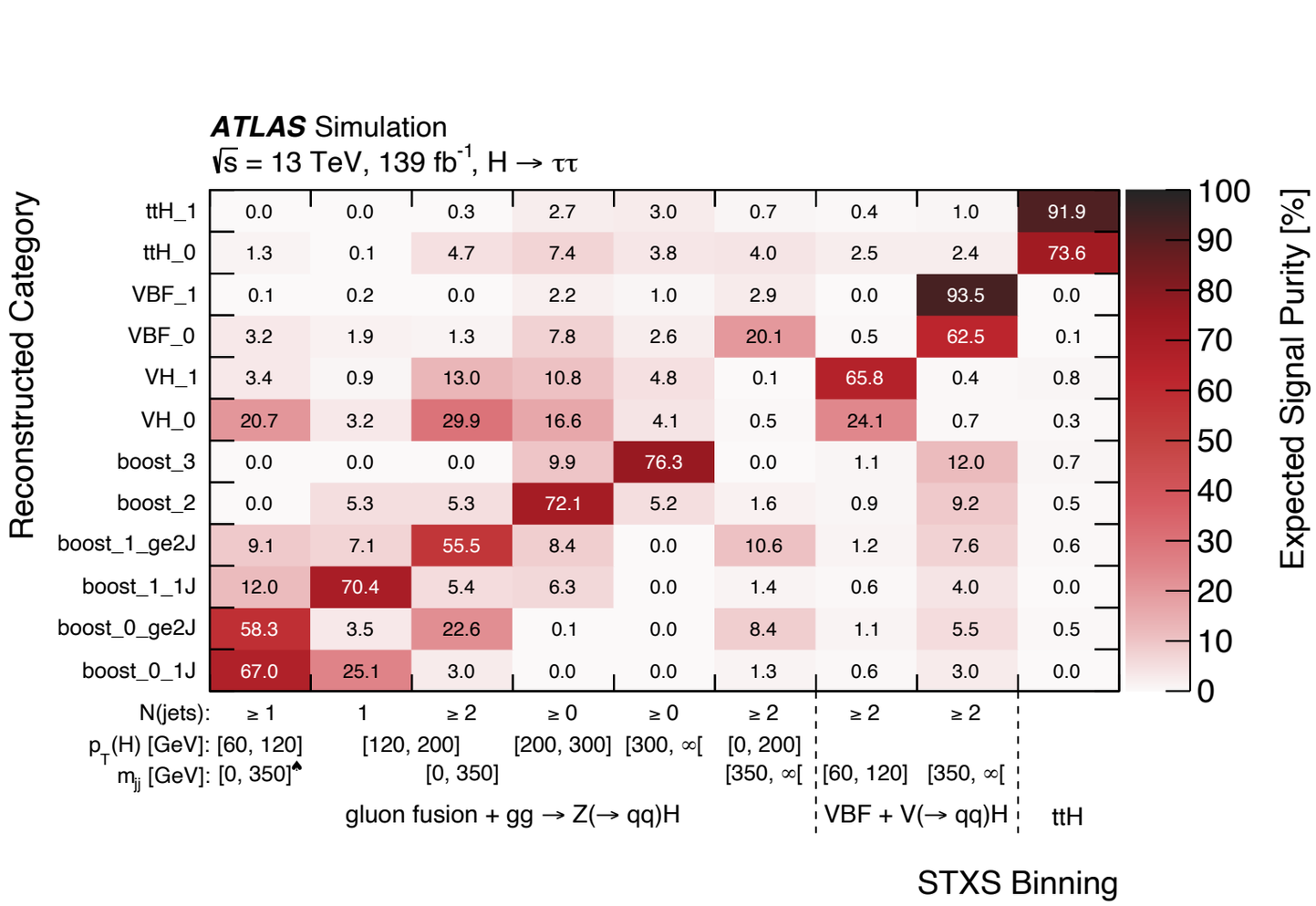

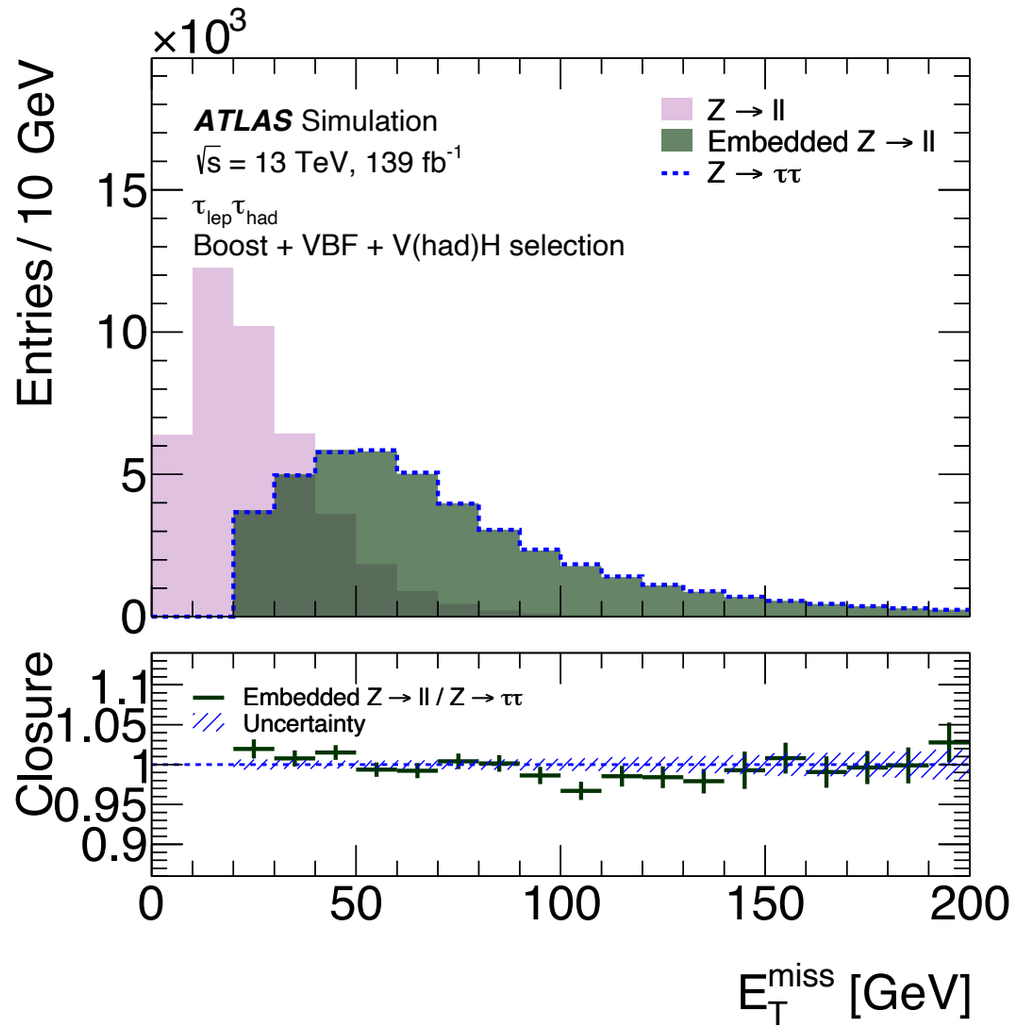

JHEP 08 (2022) 175

$H \to \tau\tau$

- Results from fitting $m_{\tau\tau}^{\mathrm{MMC}}$ in signal & control regions:

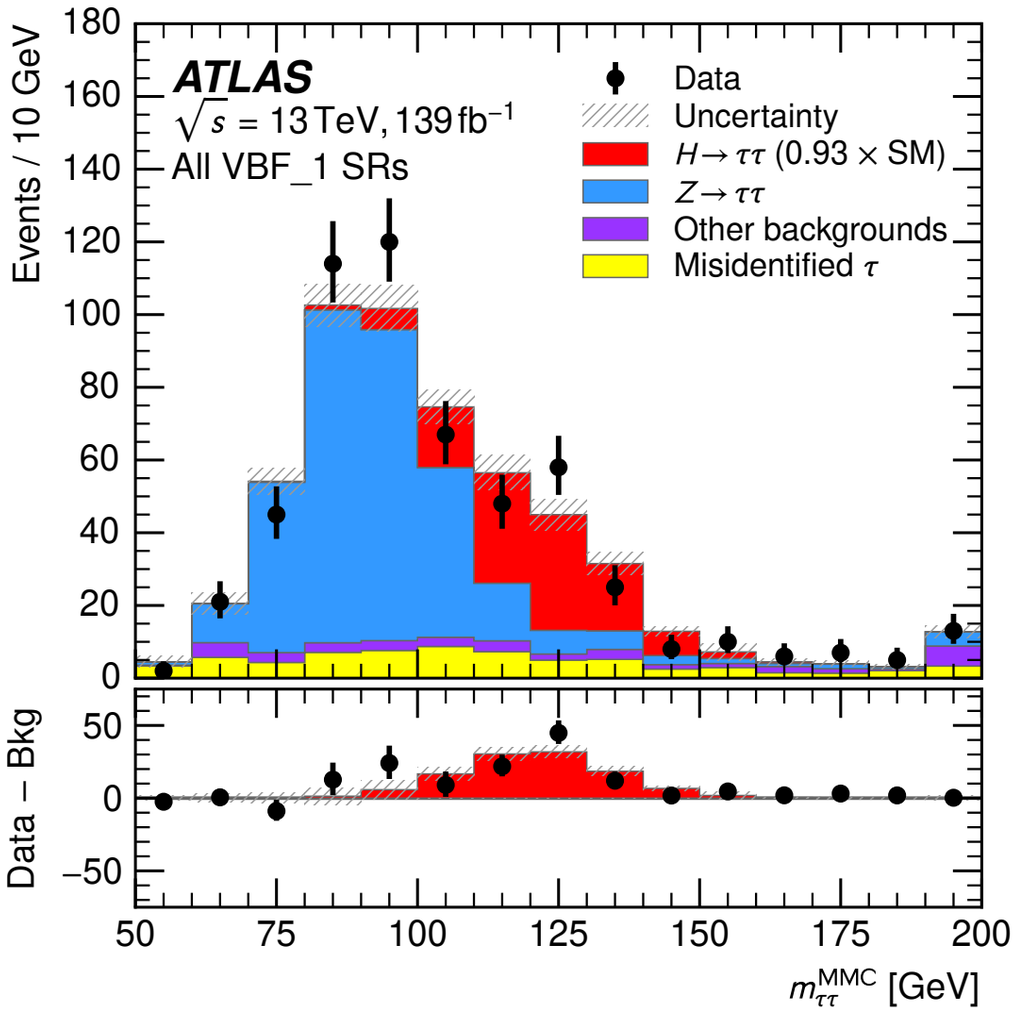

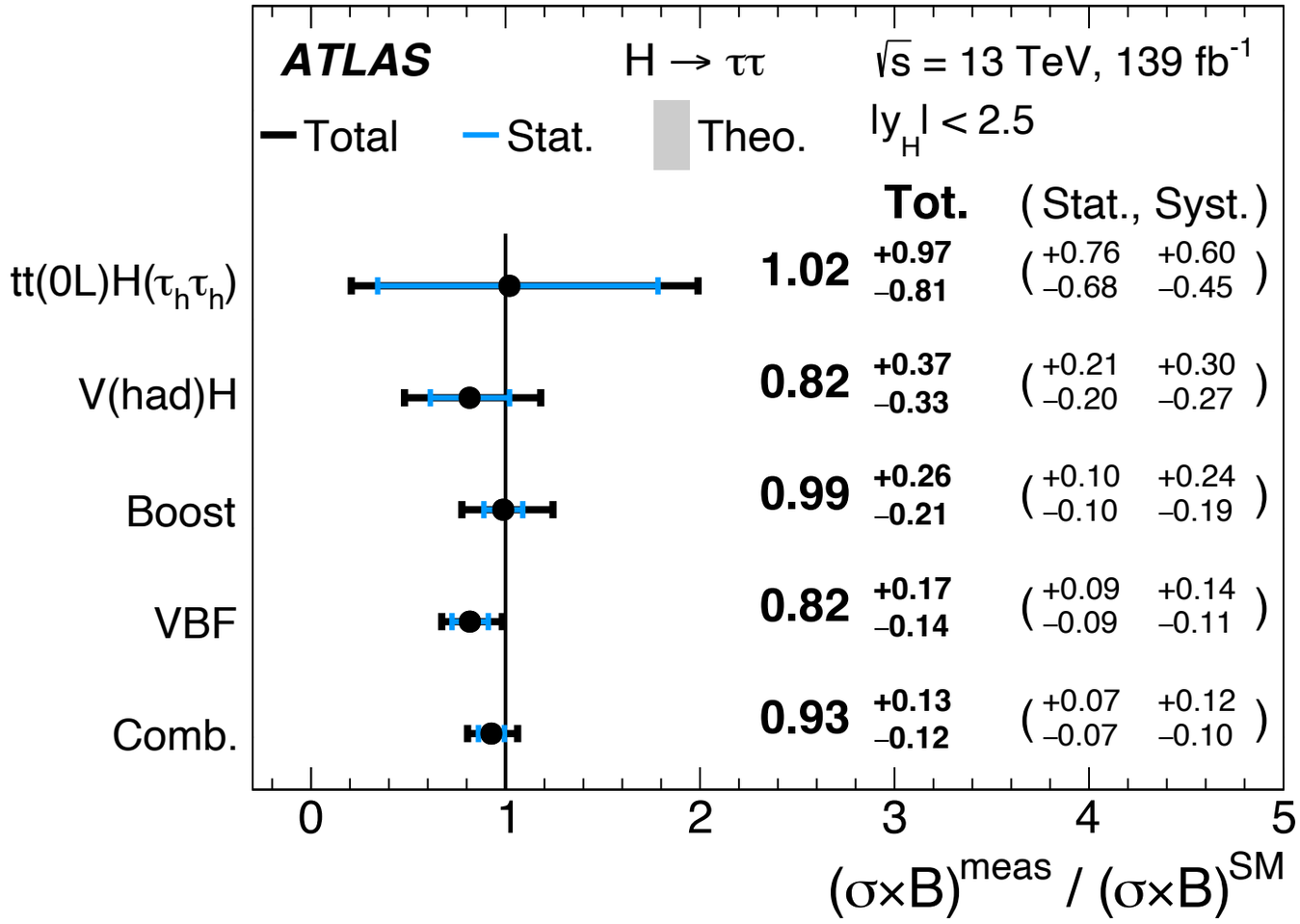

JHEP 08 (2022) 175

$H \to \tau\tau$

- Results from fitting $m_{\tau\tau}^{\mathrm{MMC}}$ in signal & control regions:

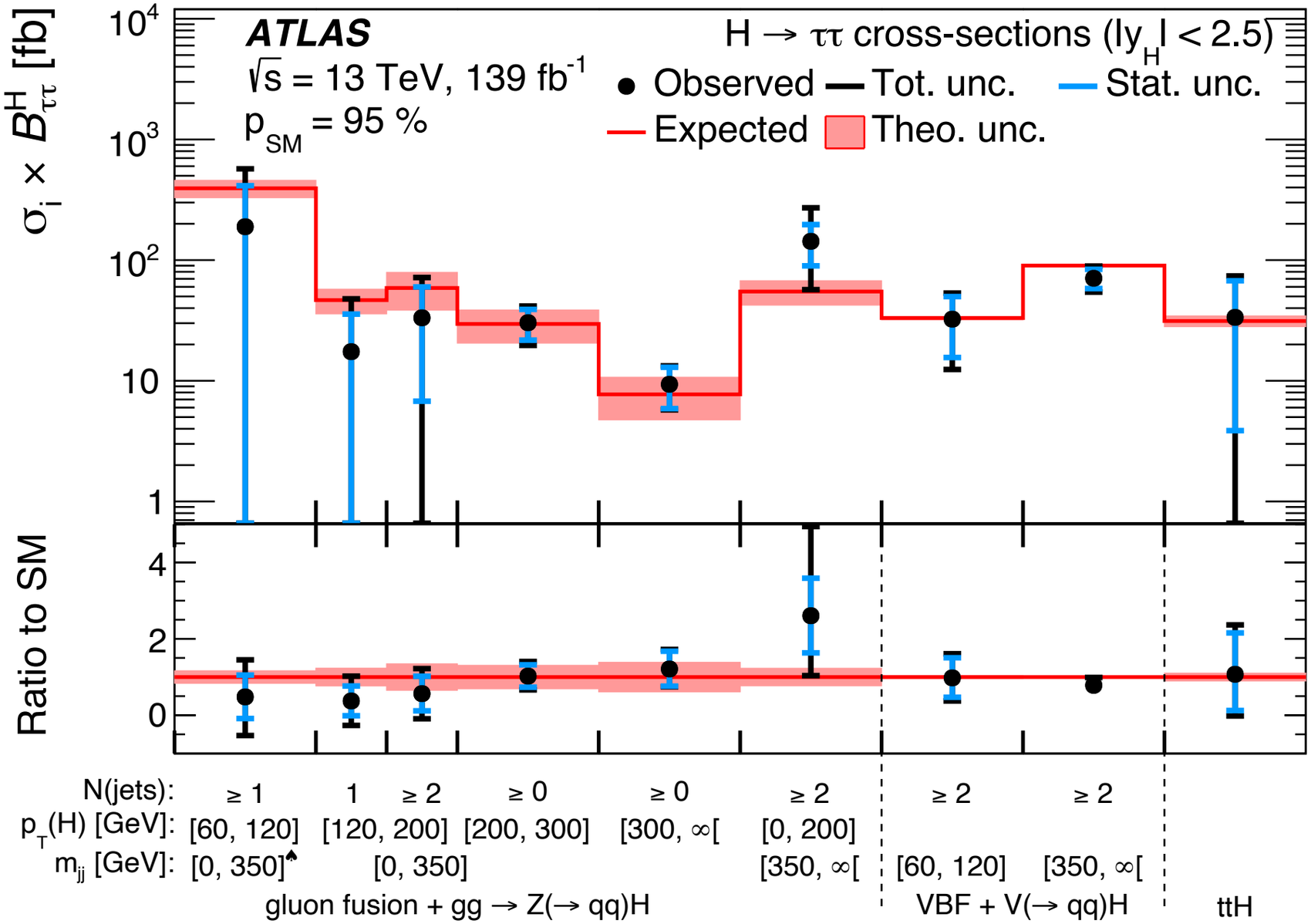

JHEP 08 (2022) 175

$H \to ZZ/\gamma\gamma$ differential cross-sections

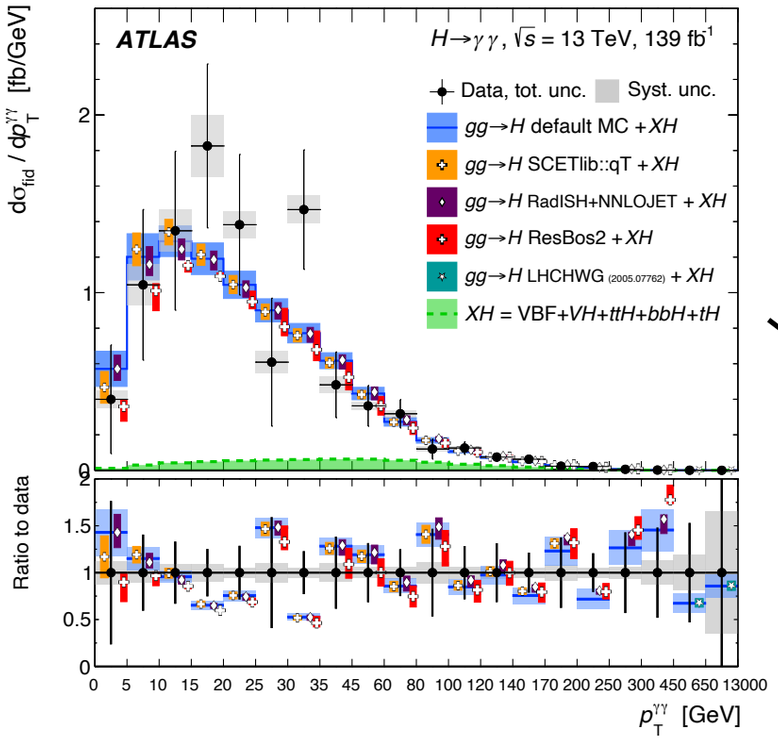

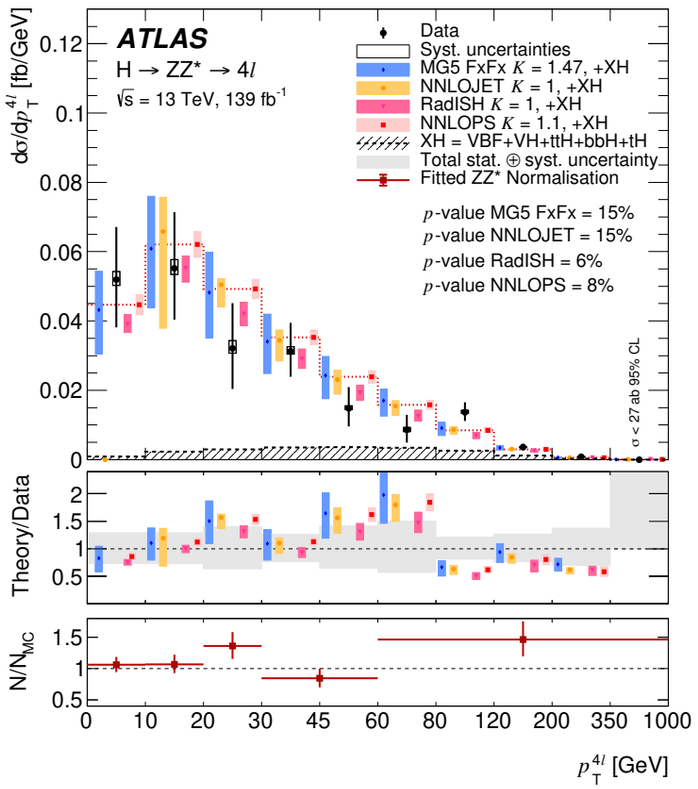

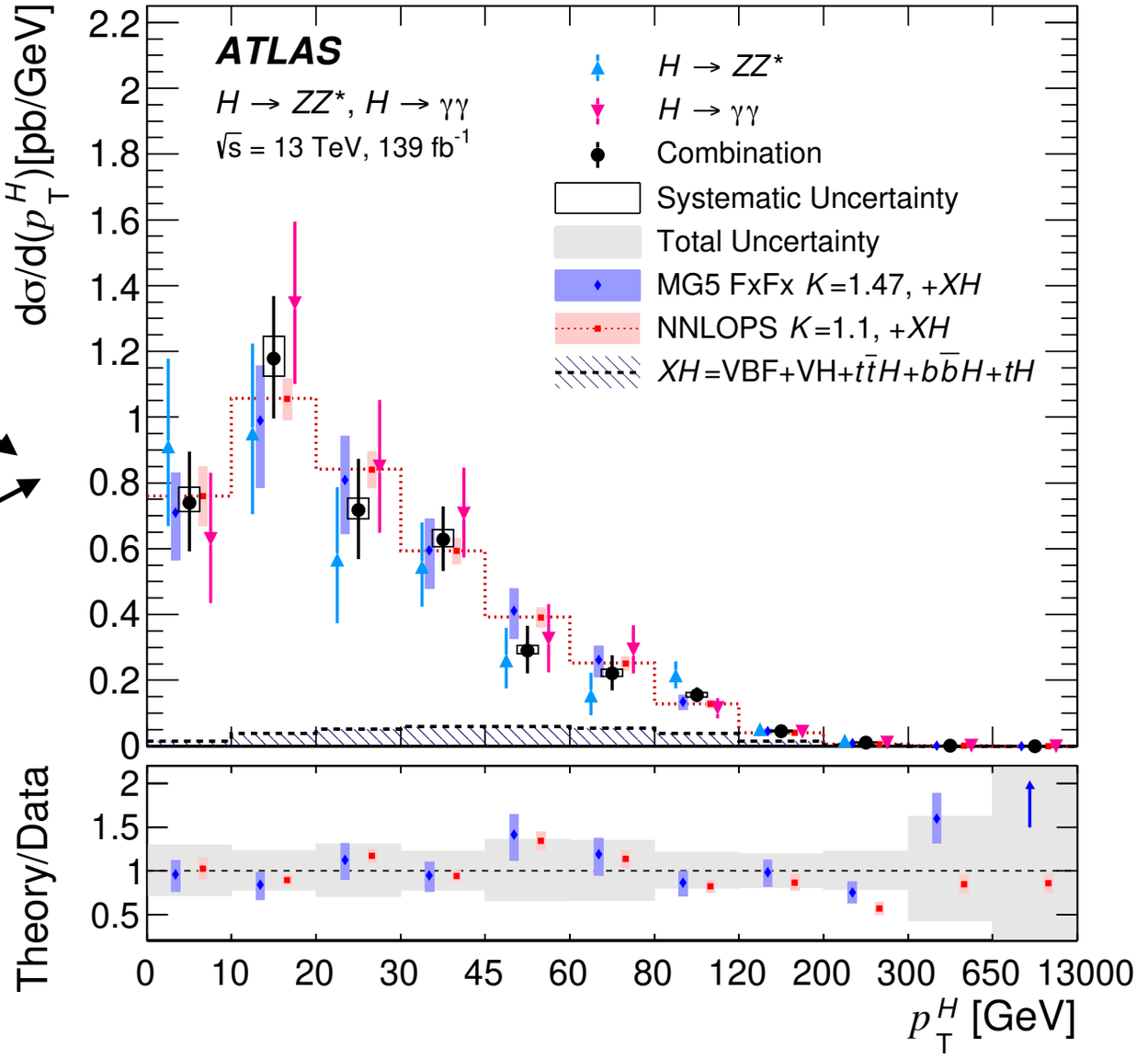

EPJC 80 (2020) 942
JHEP 08 (2022) 027
arXiv:2207.08615

Combined EFT constraints

- In operator space, there are “flat directions”, where the measurements have little sensitivity. EFT fit is therefore done using linear combinations of operators in the directions of experimental sensitivity:

$$\mathcal{L}_{\mathrm{EFT}} = \mathcal{L}_{\mathrm{SM}} + \sum_{i,D} \frac{C_i^D}{\Lambda^{D-4}} O_i^D,$$

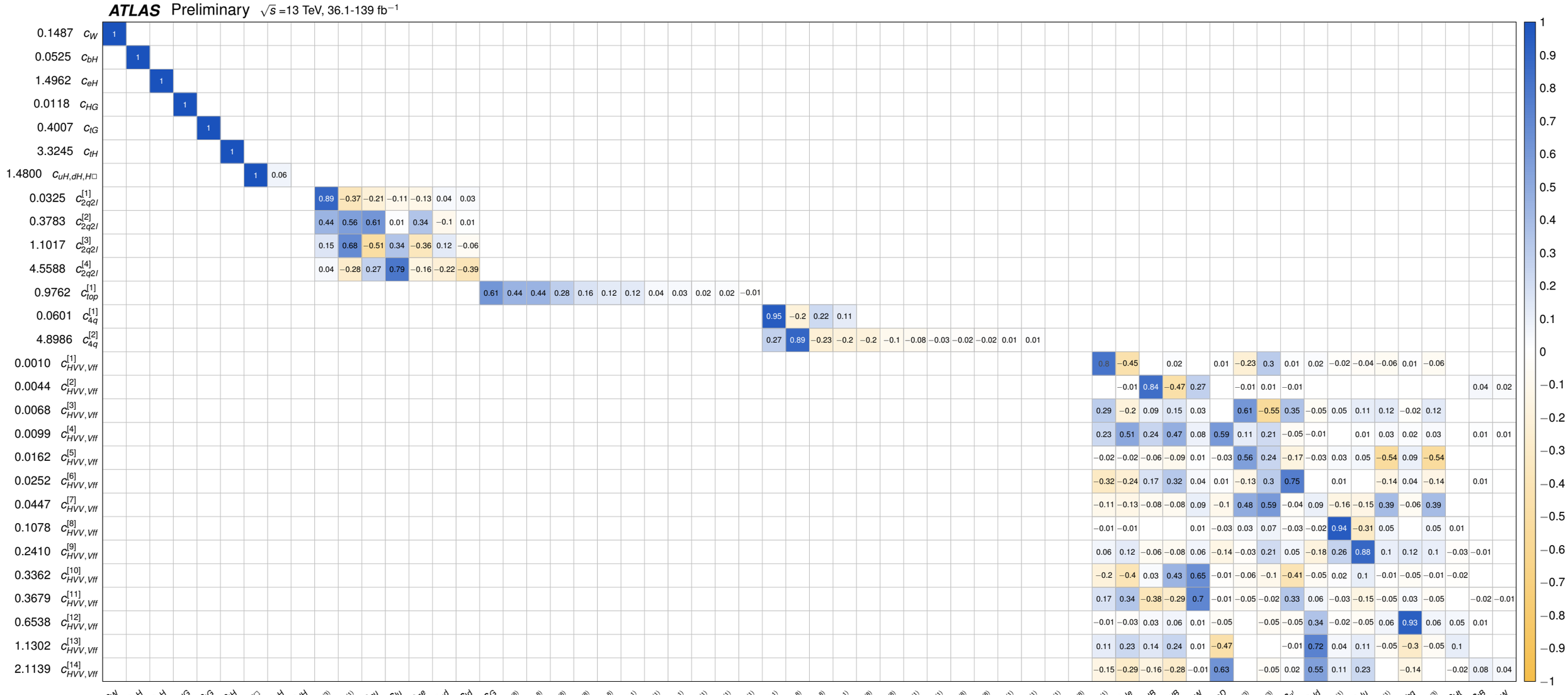

ATL-PHYS-PUB-2022-037